June 2019

Encapsulation of Organic Thermochromic Materials with Silicon Dioxide

Mingyang Huang
University of South Florida, hmychina@gmail.com

Encapsulation of Organic Thermochromic Materials with Silicon Dioxide

by

Mingyang Huang

A thesis submitted in partial fulfillment
of the requirements for the degree of
Master of Science in Materials Science and Engineering
Department of Chemical and Biomedical Engineering
College of Engineering
University of South Florida

Major Professor: Elias K. Stefanakos, Ph.D.
Venkat R. Bhethanabotla, Ph.D.
Sesha S. Srinivasan, Ph.D.

Date of Approval:
June 7, 2019

Keywords: Thermochromism, Inorganic Coating, Dye Synthesis,
In-situ Encapsulation Method, Powder Material

Table of Contents

List of Tables

iii

List of Figures

Abstract

Currently, functional materials are attracting considerable attention in the effort to solve some tough challenges the world is faced with. Thermochromic (TC) materials have the potential to make buildings more energy efficient because of their ability to change color (i.e black to white) at specific temperatures. Using this property, TC materials can reflect solar radiation in the summer, to keep a building cool during daytime hours, and absorb solar radiation in the winter to keep the building warm when their color is dark. Very often, to increase their durability, thermochromic materials are encapsulated. In this work, a new process has been developed to encapsulate low temperature TC materials with silicon dioxide. The encapsulated TC material has been characterized by several methods to determine its performance, such as SEM and TEM to determine the SiO_2 shell structural properties, TGA and DSC to test its thermal properties. The as developed SiO_2 encapsulated thermochromic materials demonstrated the color transition at around 31^oC.

Chapter 1: Introduction

1.1 Introduction

The rapid development of smart materials has encouraged researchers to explore new possibilities. The market for chromic materials is rapidly growing because of their optical, storage and color changing properties under different stimuli. Examples of such materials are thermochromic inks [1], electrochromic windows [2], and photochromic fibers [3]. Even though different chromic materials change color by different stimuli, the mechanism for such changes is similar, that is, a reversible electron or ion transfer. Generally, electrons need energy to overcome a potential barrier (ΔE) to complete the transfer and this can be provided by photons, heat or electric potential. The TC chemicals also need to be metastable for the process to be reversible [4].

The family of color change materials has expanded greatly over the past few years, especially with the development of novel micro and nanomaterials. A schematic created by Daniela Nunes shows the historic development of chromogenic materials [5].

1
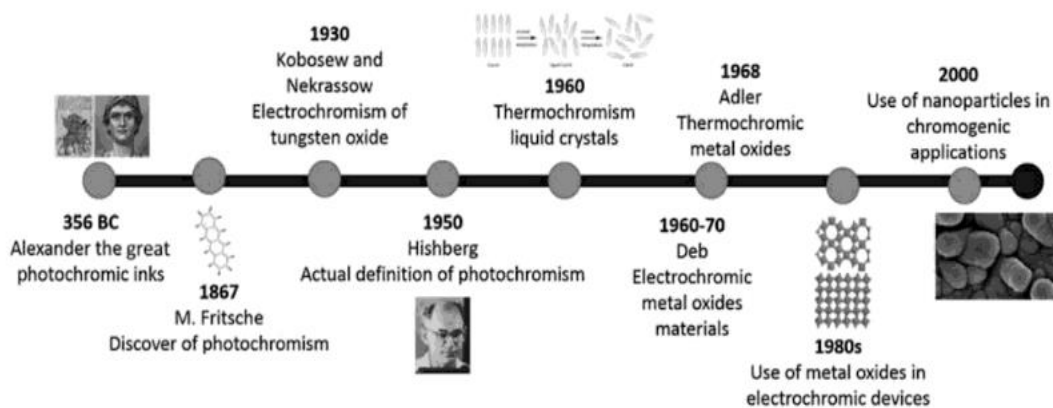
Figure 1. Historic development of chromogenic materials [Adopted from Metal Oxide Nanostructures: Synthesis, Properties and Applications by Nunes, D., Pimentel, A., Santos, L., Barquinha, P., Pereira, L., Fortunato, E. and Martins, R, 2018. Copyright 2019 by Elsevier. Reproduced with permission.]

Photochromic materials are the first chromogenic materials referenced and go back to ancient times. Warriors painted photochromic materials on their bracelets to change the color under sunlight [5]. In the 18th century, photochromism was also the first color change property that was studied and reported. Fritsch observed that tetracene is colored in the dark, becomes colorless in the sunlight and is reversible [6]. However, the word photochromism, which comes from Greek, was created in 1950 by Fritsch to describe color change phenomena with a light stimulus. After that, more words related to chromism were created to describe different new types of color change phenomena.

At this time, the field of chromism has significantly expanded because of the popular use of nano-synthesis techniques in different fields. Nanostructures are more advanced than thin film structures because they have larger surface area and higher surface to volume ratio, that can enhance the material's performance [5]. Furthermore, the applications of chromogenic materials is growing very fast. Thermochromic (TC) materials, and especially organic, often need to be protected from external interactions and stimuli. The purpose of this thesis is to develop a process to encapsulate thermochromic dyes with silicon dioxide (SiO_2). A sequence of

2

experiments is described in the effort to achieve this goal. The results are analyzed, and conclusions are drawn for various applications and future research.

1.2 Problem Statement and Objectives

Substantial amount of information is available on new chromic materials that can be used in a few applications and energy conservation for global sustainability, energy conservation being equally as important as energy generation. Buildings use 30%-40% of the global energy consumption [7, 8]. Even automotive cooling and low-cost lighting systems can help save energy, energy consumption still increasing because of city heat island phenomenon [9]. Higher ambient temperatures not only affect the energy consumption, but also have a negative impact on human health. In fact, over 400 large overheated cities are documented around the world [10, 11]. To counterbalance the effect of urban overheating, numerous mitigation projects have been developed. Recent attention has focused on using high sunlight rejection materials (cool roofs) to reduce the amount of solar energy absorbed [12]. In addition, construction materials play a crucial role in the thermal behavior of urban areas as well as a building's energy consumption and indoor environment quality. If one views heat-absorbing material as first-generation material, then cool materials (heat reflective) and fluorescent materials (photoluminescence) can be thought of as second and third generation materials [13]. Highly reflective cool roofs can decrease solar energy absorption, lower the surface temperature and provide energy savings during the summer [14]. However, they are not effective for all seasons or for cold climates and can even contribute to higher energy consumption by rejecting solar energy. Thermochromic materials can be used in place of just reflecting or absorbing materials for energy savings throughout the year in all climates. [15, 16]. A common drawback of organic thermochromic

3

materials is their degradation when exposed to ultraviolet radiation [17]. Surface protection from such radiation is therefore significant.

Recently, different microencapsulation methods of thermochromic materials have been reported. Different types of polymers and several layers have provided longer TC material life span. [18]. It also helps to protect the thermochromic material from contaminations and component subliming. But the UV light can still destroy any organic thermochromic system [19]. Wan Zhang reported that the encapsulation of a thermochromic material by amorphous silica could protect it from UVB light (290-320nm) [20]. This thermochromic material, however, is not suitable for a building's surface coating, because it's color change temperature is about 60° C [20]. Ye et al reported a thermochromic material, coated by the polymer poly(N-isopropylacrylamide), that could change its color around 32° C, but it does not satisfy the needs because it changes from transparent to opaque and may be suitable just for windows [21].

For better performance, encapsulation of thermochromic materials by metal oxides is a suitable solution. Results on the encapsulation of a black leuco dye purchased from a company or a blue leuco dye prepared in our lab are presented in this work.

1.3 Thesis Outline

Chapter 2 describes the fundamental knowledge about color chromism, photochromism, electrochromism, and thermochromism, some related researches and applications are stated to help everyone get a better understanding.

Chapter 3 explains the experimental methodologies and the reactions during the experiments, it also illustrates the mechanism for encapsulation of both a commercial dye and lab-synthesized dye.

4

Chapter 4 discusses details of various analytical and metrological characterization techniques used to determine the encapsulating layer characteristics and help develop the experimental process. The main characterization tools used are SEM-EDS, TEM, DLS, TGA and DSC. Both surface morphology and thermal behavior can be analyzed via these techniques.

5

Chapter 2: Background and Literature Review

2.1 Color Chromism

The ability of the human eye to detect colors is based on a certain range of electromagnetic wavelengths sensitive to cells in the retina. Visible light is in the wavelength range of 380 nm to 740 nm. Sunlight that contains electromagnetic wavelengths from 290 nm to 3200 nm is incident on the material surface, part of it is transmitted and part of it is absorbed by the material, with the remaining reflected. Sometimes, an object will not just reflect radiation but also emit radiation presenting a colorful picture.
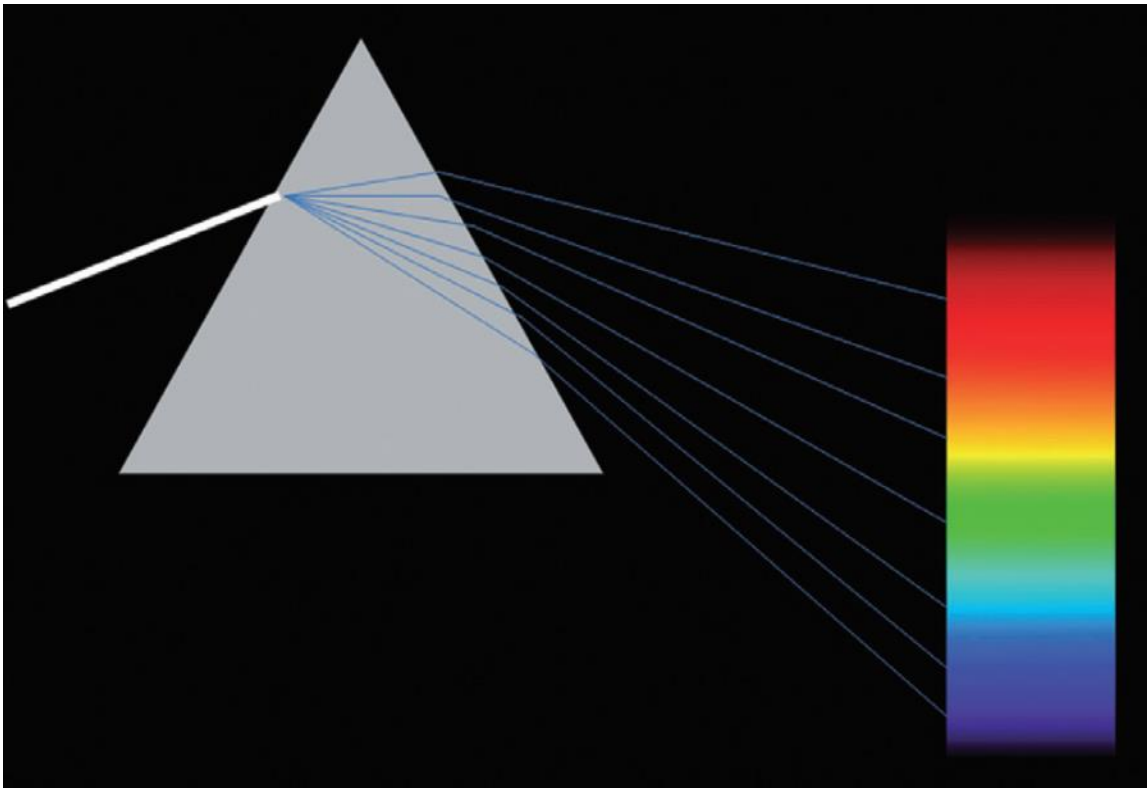
Figure 2. A narrow beam of sunlight passing through a prism with different wavelengths separated due to refraction. [Adopted from Color: An Introduction to Practice and Principles, by Kuehni, Rolf G, 2012, copyright by Hoboken, N. J., Wiley. Reproduced with permission.]

6

Electromagnetic radiation consists by wave packets of discrete energy called photons The energy of a photon is proportional to the frequency of the electromagnetic radiation. Since photons can be absorbed or emitted by charged particles, photons assume an important role in the transmission of energy. According to the Planck-Einstein relationship, the energy of a photon is $E=h\nu$ where h is the Planck Constant and ν is the frequency. When a photon is absorbed by an atom, it also excites its bound electrons, raising the energy level of the electron.

2.2 Photochromism

First-time photo chromism was discovered in the 1880s and was identified as a reversible color change, caused by ultraviolet (UV) electromagnetic radiation, that has undergone a chemical reaction [23]. Recently research intensified focusing on the design and synthesis of a photosystem in the field of biosensing. [24]. Furthermore, functional materials that can be used in different applications, such as ion sensing, supramolecular chemistry, and data storage, have had important commercial impact.

In analytical chemistry, researchers have developed a number of chemical sensors for sensing inorganic ions based on Photochromism [25]. It is both of interest and challenge to study biosensing systems. Some common compounds like spiropyrans and azobenzenes can be used as the dye for a photochromic system; their structure can switch due to different light wavelengths under UV and Visible excitation. Figure 3 shows two different structures of spiropyrans and azobenzenes [24], illustrating a reversible process.

7
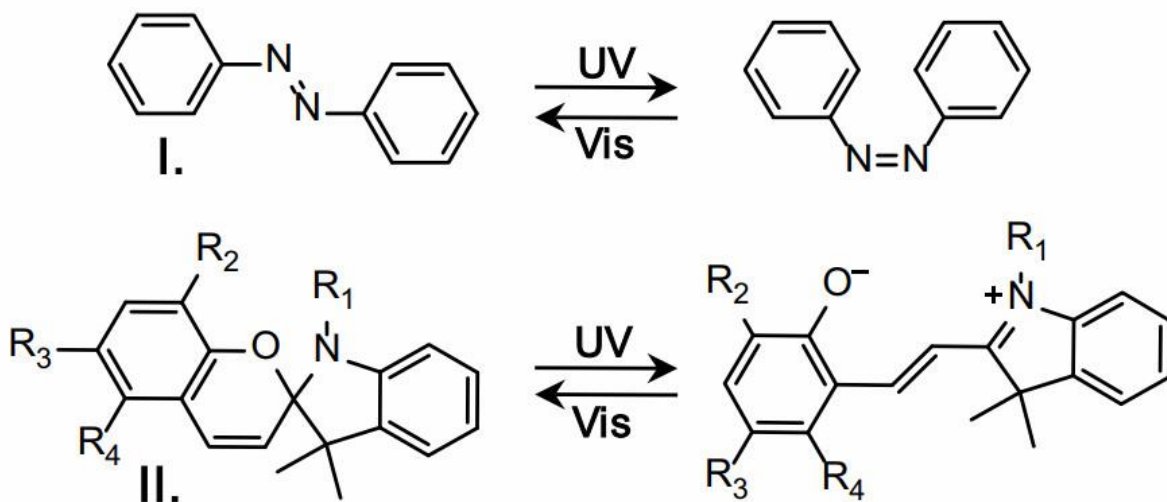
Figure 3. I and II are the different structures of azobenzenes and spiropyrans. [Adopted from Towards photochromic and thermochromic biosensing, by Avella-Oliver, M., Morais, S., Puchades, R., & Maquieira, Á, 2016, *TrAC Trends in Analytical Chemistry*, 79, 37-45. Copyright 2016 by TrAC Trends in Analytical Chemistry, Reproduced with permission.]

2.3 Electrochromism

Electrochromism (EC) is a phenomenon in which the material can change color in response to an electric potential (voltage change). Due to their special reversible optical change, electrochromic devices are broadly applied in fields of energy, automotive industry and satellite thermal control [26]. Essentially, the EC device is a rechargeable capacitance, with the electrodes separated by different kinds of liquid or solid electrolytes, and the optical color change occurring. A problem called 'memory effect' sometimes occurs when a pulse of current decays the device and the new redox state persists resulting in weak performance. Figure 4 shows the configuration of an EC device. This EC device can work both in the reflective and transmissive mode. [26].

8
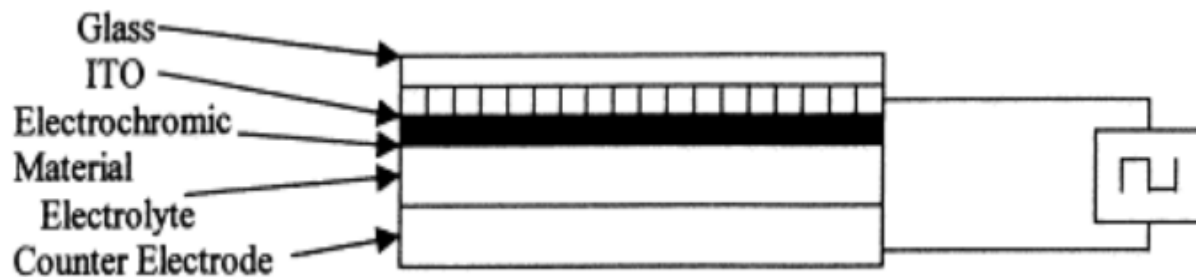
Figure 4. Schematic diagram of an electrochromic device [Adopted from Electrochromic material and devices: present and future, by Somani, P. R., & Radhakrishnan, S, 2003, *Materials chemistry and physics*, *77*(1), 117-133. Copyright 2002 by Elsevier Science B.V. Reproduced with permission.]

Electrochromic materials can be organic and inorganic. Inorganic electrochromic materials usually contain transition metal oxides and have better stability with wider temperature and voltage range [27]. Organic electrochromic materials have certain advantages because they can be easily modified and have lower cost. Novel nanocomposites consisting of metal oxides and organic molecules can be produced by low-cost sol-gel methods. Under an applied voltage, the inorganic EC material can inject or extract electrons during reversible redox reactions. The EC performance is controlled by the switch that controls in turn the speed of electrons and/or ions during the redox reactions [28, 29, 30].

2.4 Thermochromism

Thermochromic (TC) materials change color at two different temperatures [26]. They also exist in nature [31]. Organic thermochromic materials are more commonly found in commercial products. Usually, the thermochromic material's color change can be triggered by heat applied to the intrinsic system. A thermochromic system usually contains three components: a dye, a color developer, and a co-solvent. The dye should be pH sensitive that can transfer electrons and the color developer acts as a proton donor during the color changing process [31]. Recently, crystal violet lactone (CVL), as a dye, alkyl gallates and bisphenol A

9

(BPA) as a color developer, and alcohols as co-solvent are of major research interest [32] This thermochromic system can change color from blue to white as the temperature increases. The benefit of this organic dye system is its low critical point (color change temperature), low cost and no toxicity.

For the three component thermochromic system, the interaction between dye-developer and developer-solvent happens during the color changing process [33]. The CVL will change its structure (bonding change) by transferring an electron during the reaction. Figure 5 has been used in many papers to show the ring-closed Spiropyran (SP) form which is colorless, and the ring opened Merocyanine (MC) form which is blue. Also, Bourque and White (2014) discovered that the molar ratio of these three components could result in different color transformations, such as dark to light and light to dark [32].
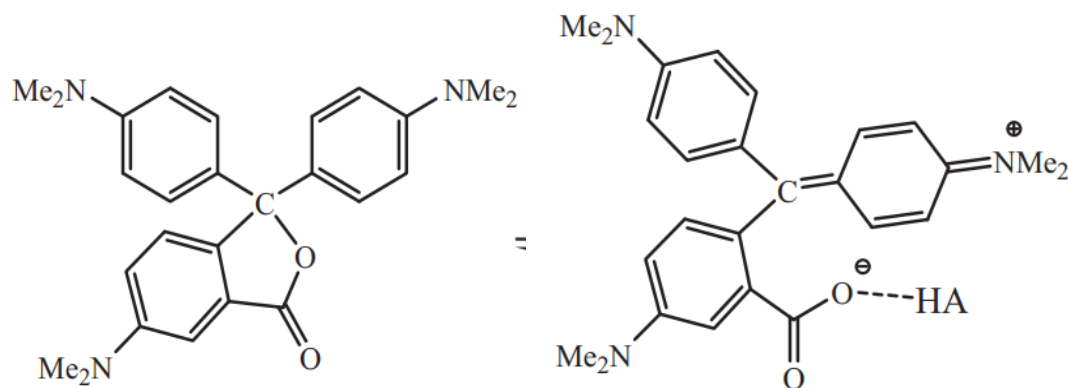
Figure 5. The ring-closing and ring-opining form of CVL. The SP form on the left and the MC form on the right. [Adopted from Control of thermochromic behaviour in crystal violet lactone (CVL)/alkyl gallate/alcohol ternary mixtures, by Bourque, A. N., & White, M. A, 2014, *Canadian Journal of Chemistry*, *93*(1), 22-31. Copyright 2014 by Canadian journal of chemistry. Reproduced with permission.]

Chapter 3: Encapsulation of Thermochromic Materials

3.1 Background

Due to its changing color, the thermochromic (TC) material can be used to change the absorption and reflection properties of a surface. This can potentially enable transfer of thermal energy into a building resulting from solar radiation [36]. Thus, lower surface temperatures can be achieved by increasing the reflectance of the surface and higher temperatures by increasing the surface absorption. However, because the leuco dye and color developer are organic materials, they can easily degrade under solar radiation. Researchers have studied various methods of polymer TC material encapsulation to enhance its thermal stability. According to Nassau (2001), a dye can undergo photodegradation under sunlight when ultraviolet light interacts with the chemical bonds and destroys the chromophores in the dye [37]. It is therefore can be important to encapsulate the TC material with an inorganic metal oxide such as SiO_2 or ZnO.

3.2 Mechanism

Usually, three steps are needed to complete the *in-situ* encapsulation process: emulsification of thermochromic core, outer material capsule formation, and curing process. The mechanism of encapsulation uses an emulsion technique to create stable small droplets in a solution. The SiO_2 will collide and self-assemble on the surface of the dye in a vigorous stirring environment. An emulsifier is key to creating a homogeneous dye particle dispersion and stable Oil/water(O/W) emulsion. Vigorous stirring is another key to make the droplets as small as

11

possible to increase the performance of the TC material [38]. The use of a commercial dye,that has been coated with a polymer, makes it difficult to control the particle size since it is already set during manufacturing. Also, the commercial dye comes as a powder which means it will form a sol while it is dispersed in the solution. Both sol and emulsion are a type of colloid. Another choice is making a new TC material by melting CVL, BPA, and solvent in a bath and adding it into a water solution. The benefit of this is to produce smaller particle sizes, but the drawback is a more difficult extracting and drying process. Figure 6 shows the synthesis strategy for the emulsion and sol process.

3.2.1 Emulsion Process

When two immiscible liquids are mixed, Figure 6A, the oil phase composition will be dispersed like in Figure 6B when shaking, stirring and ultrasonic vibration are applied. However, this mixture is unstable and the oil droplets will aggregate (Figure 6C). To form a stabilized emulsion solution (Figure 6D), an emulsifier or surfactant are needed to lower the surface tension between the two phases.
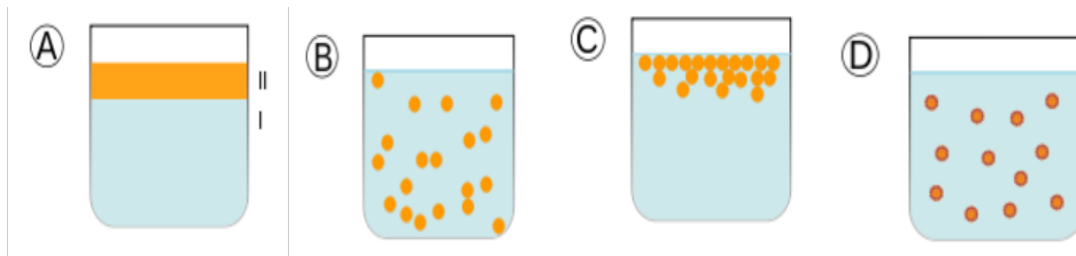
Figure 6. Synthesis strategy for the emulsion process. A. Separated immiscible liquids; B. Immiscible liquids after shaking, stirring and ultrasonic vibration; C. Two immiscible liquids after settling; and D. Two immiscible liquids after the addition of a surfactant

In general, surfactants, which are usually organic compounds that contain both hydrophobic and hydrophilic groups at their tails and heads separately, can be classified as two different types: ionic and nonionic [39]. The head-tail structure offers the surfactant the ability to

12

enable solubility to both oil and water (Figure 7), which means it will adsorb at the interface between the oil and water molecules and prevent aggregation of oil in water. The classification depends on the main group when the ionic surfactant contains anionic, cationic and zwitterionic groups. In different encapsulation processes, different ionic surfactants are used to enhance the solution's stability and encapsulation performance.
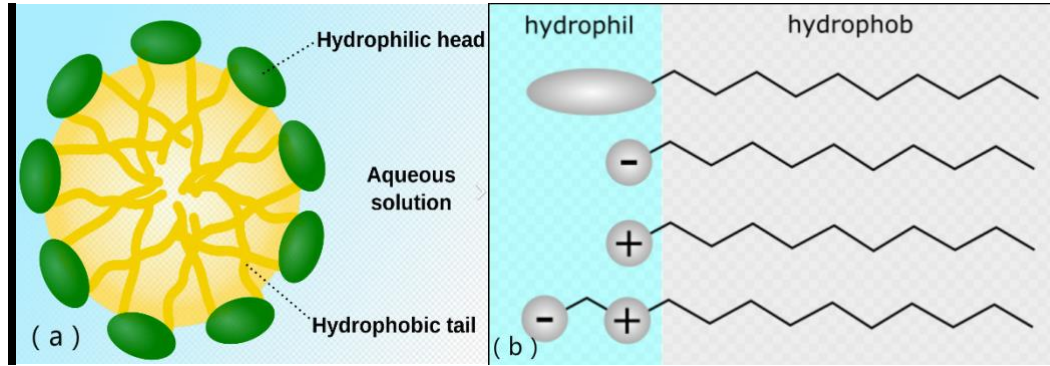
Figure 7. (a) Head-tail structure of surfactants; and (b) different types of ionic surfactants.

3.2.2 Silicon Dioxide Precursor Mechanism

For the SiO_2 encapsulation, following the Stöber process published in 1968 [40], tetraethyl orthosilicate (TEOS) is used as the precursor. Because, it can easily hydrolyzed

$$Si(OC_2H_5)_4 + H_2O \xrightarrow{NH_3} SiO_2 + 4C_2H_5OH \tag{1}$$
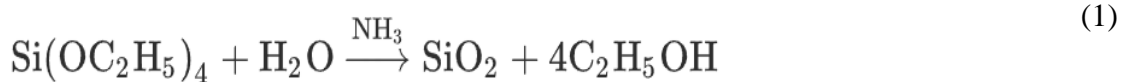
to form SiO_2 particles with ammonia as catalyst as given in equation (1). It is a one-step approach to preparing monodisperse spherical silicon dioxide particles. The details of the SiO_2 formation is TEOS will be hydrolyzed in the presence of ammonia as shown in formulations (2) and (3). As a result, a mixture of ethoxysilanols ($Si(OH)_4$, $Si(OEt)_3OH$,

$$Si(OEt)_4 + H_2O \longrightarrow Si(OEt)_3OH + EtOH \tag{2}$$

$$Si(OEt)_4 + 2H_2O \longrightarrow Si(OEt)_2(OH)_2 + 2EtOH \tag{3}$$

13
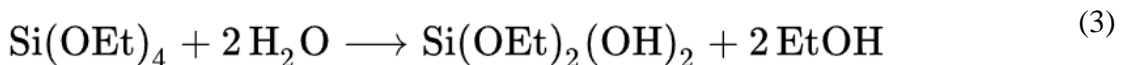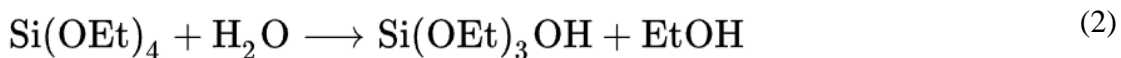
Si(OEt)$_2$(OH)$_2$, and Si(OEt)(OH)$_3$) will be formed and it will further condense with silanol or TEOS to lose the water. The reactions of formation are shown below (4), (5) and (6).

$$2\,Si(OEt)_3OH \longrightarrow (EtO)_3Si-O-Si(OEt)_3 + H_2O \qquad (4)$$

$$Si(OEt)_3OH + Si(OEt)_4 \longrightarrow (EtO)_3Si-O-Si(OEt)_3 + EtOH \qquad (5)$$

$$Si(OEt)_3OH + Si(OEt)_2(OH)_2 \longrightarrow (EtO)_3Si-O-Si(OEt)_2OH + H_2O \qquad (6)$$
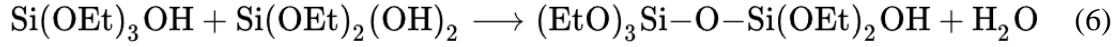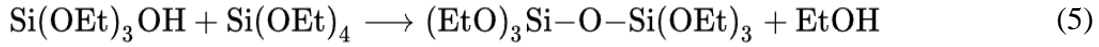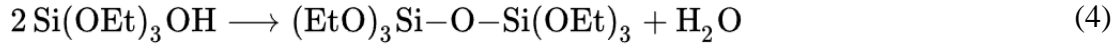
Based on further hydrolysis of the ethoxy group which leads to the crosslinking structure of Si, O, and OH group, silicon dioxide (SiO$_2$) powder is produced. The reason of this one-step approach is because the condensation and hydrolysis reaction happen simultaneously [40]. The simplified process diagram can be described as shown in Figure 8. The final particle size ranges from 50 to 1000 nm, and is controlled by the concentration, types of catalysis, temperature and co-solvent applied. Van Helden et al state that the particle size will be increased along with the water and ammonia concentration, but with a broader range of size distribution. However, the TEOS concentration has an inverse impact on the final particle size, a higher concentration resulting in smaller particle sizes because of the bigger number of nucleation sites [41].

14
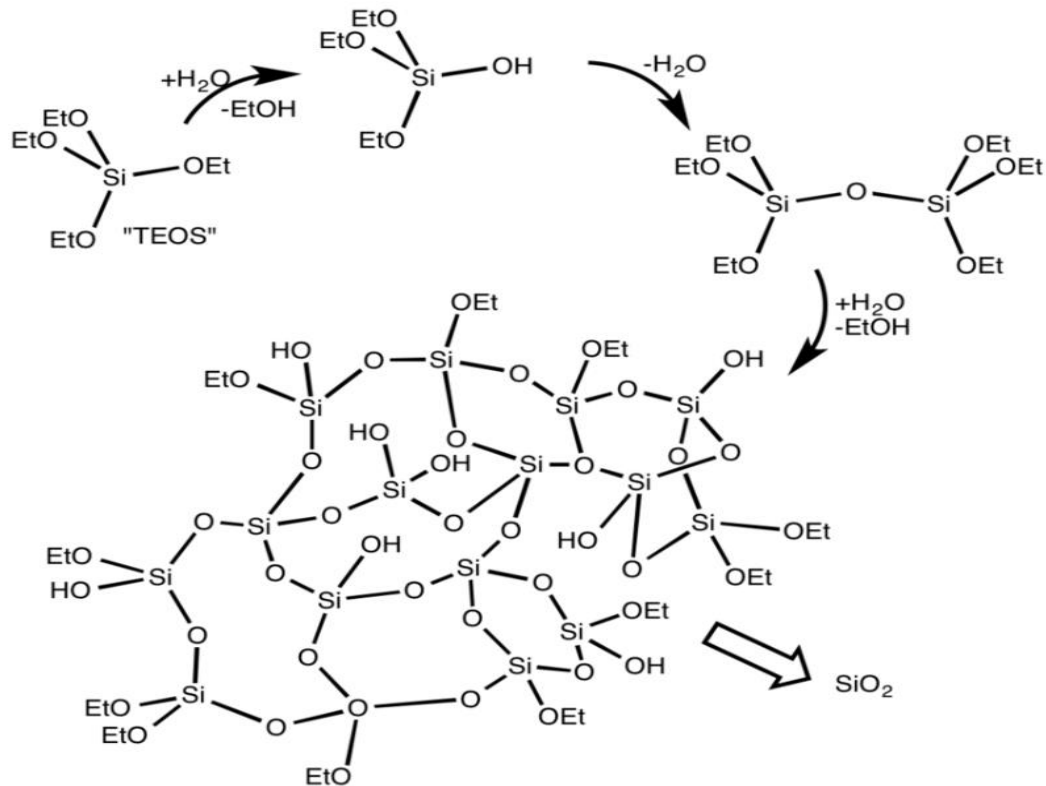
Figure 8. The Stöber process that uses TOES to form silicon dioxide. [Adopted from Controlled growth of monodisperse silica spheres in the micron size range, by, Stöber, W., Fink, A., & Bohn, E, 1968, *Journal of colloid and interface science*, *26*(1), 62-69. Reproduced with permission.]

3.2.3 Silicon Dioxide Encapsulation Mechanism

The purpose of encapsulation is to form the silicon dioxide on the surface of the core material. As indicated in Figure 9, while an anionic surfactant, alkylbenzene sulfonates (SDBS) is added into the solution of water and dye particles [42]. There, it will be absorbed and will surround the dye due to its hydrophobic tail and hydrophilic head structure. The surface of the dye becomes a negative charge, based on the SDBS's head structure. Due to the electrostatic attraction, catalyzed amine will adsorb on the dye surface as well. This hydrophobic micro field allows the TEOS or ethoxysilanols to approach the dye surface. Under these conditions, with the promotion of the catalyst, silicon dioxide can be generated and encapsulated on the surface of

15

dye by the Stöber process, shown as formulation (1) Figure 9. The particle size change during the experiment are shown in Figure 9 as well.
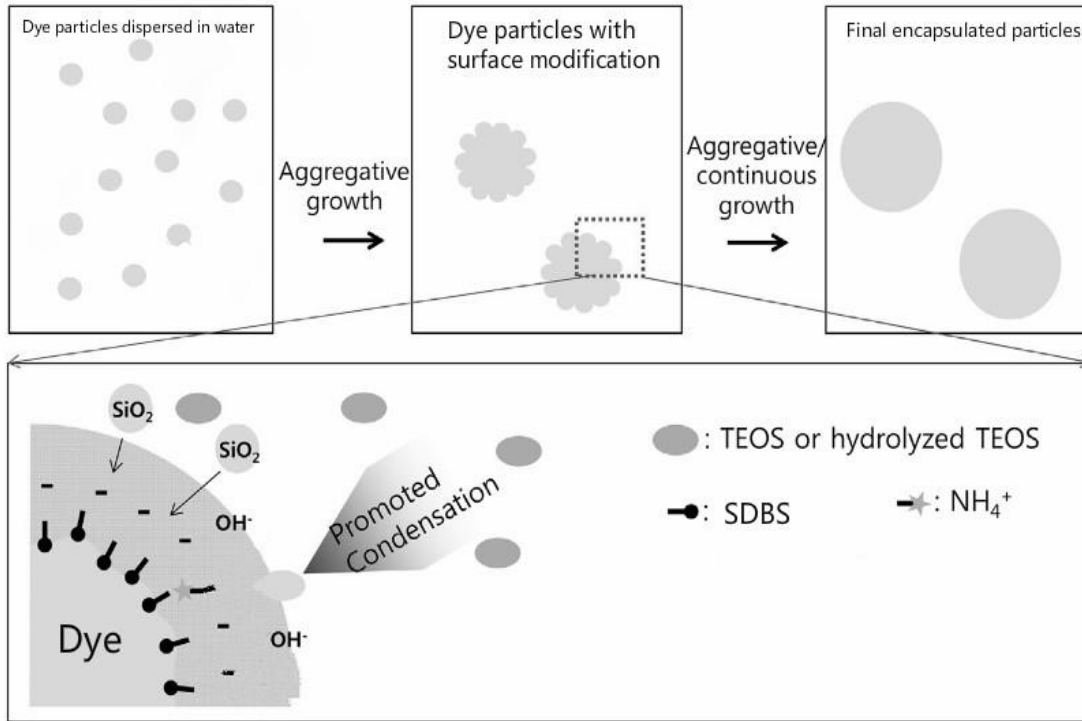
Figure 9. Schematic representation of the particle structure during the encapsulation [Adapted from Synthesis of uniform silica particles with controlled size by organic amine base catalysts via one-step process, by, Han, J., Yu, T., & Im, S. H, 2017, *Journal of industrial and engineering chemistry*, *52*, 376-381. Copyright 2017 by The Korean Society of Industrial and Engineering Chemistry. Reproduced with permission.]

3.3 Process of Commercial Dye with Silicon Dioxide (CDTCM at SiO_2)

3.3.1 Chemicals Used

The commercial dye that changes color at about 30° C was bought from Amazon Company. Sodium dodecyl benzenesulfonate (SDBS), Tetraethyl orthosilicate (TEOS) and Ammonia were obtained from Sigma-Aldrich.

3.3.2 Sample Preparation

A beaker is used containing 80 ml of DI Water at 70° C and stirred at.400 rpm. In this, the commercial dye (0.5g) is added. After 5 minutes, SDBS (2g) and TEOS (3ml) are added to

16

the solution at 70° C and stirred until an emulsion is formed (usually 2 hours). Then ammonia is added as a catalyst under stirring at the same temperature for an additional 2 hours. Finally, the sample is washed three times with 10% ethanol.

3.3.3 Thermal Treatment

After washing, the sample is placed in an incubator and dried at 150° C for 24 hours. Finally, the powder sample is stored in a glass tube.

3.4 Process of Blue Dye with Silicon Dioxide (BDTCM at SiO₂)

3.4.1 Chemicals Used

The blue dye (changes color at about 30° C contains 1-tetradecanol, crystal violet lactone (CVL) and bisphenol A (BPA), the surfactant sodium dodecyl benzene sulfonate (SDBS), the precursor tetraethyl orthosilicate (TEOS) and encapsulation of the catalyst ammonia are all procured from Sigma-Aldrich.

3.4.2 Sample Preparation

The blue dye solution is made first with: 25 ml 1-tetradecanol, 0.3 g CVL and 1.5 g BPA, all mixed in a beaker at 70° C and stirred at 400 rpm for one hour. At the same time, 100 ml DI water is heated to 70°C and maintained at that temperature throughout the process. Then, 4.5 ml blue dye and 1g SDBS are added into the hot DI water solution and stirred at 800 rpm. After 1hour, 3 ml of the SiO₂ precursor (i.e. TEOS) solution is added and stirred for half more hour. Finally, 2 ml ammonia is added, and the solution is turned off after 3 hours. Further cooling down and filtration is necessary to obtain a powder sample.

3.4.3 Thermal Treatment

After washing it three times, the sample was placed in an incubator at 150° C for 24 hours to dry. Finally, the powder sample is stored in a glass tube.

17

Chapter 4: Characterization

4.1 CIE Lab Color Meter

The CIE LAB color space is a color space defined by the International Commission on Illumination (CIE) in 1976. It expresses color as three numerical values, L* for the lightness and a* and b* for the green–red and blue-yellow color components. CIE LAB was designed to be perceptually uniform concerning human color vision, meaning that the same amount of numerical change in these values corresponds to about the same amount of visually perceived change [43]. For our microencapsulated thermochromic samples, we can use CIE Lab to measure the critical point which is important for its application. Also, we can detect the color difference during the heating and cooling process. Another benefit is that CIE Lab helps indicate the quality of the thermochromic material when it can measure the color contrast expressed by a corresponding F(T) value, marked as CCF (the color difference between the coloration limit point and the discoloration limit point). However, this test is not done in this thesis due to the lab instrument limitation.

4.2 SEM (Scanning Electron Microscopy)

The SU70 SEM shown in Figure 10 is used to obtain a higher resolution image. Resolution refers to the minimum distance between two feature points that the instrument can clearly distinguish. We can also calculate the resolution from the formula $R = 0.61\lambda/n \cdot \sin \alpha$. In this formula, R is the Resolution, λ is the wavelength of the electron beam, n is the index of refraction of the medium between the objective lens and the object, and α is an angle of

18

inclination. For example, the light source used in an optical microscope has a wavelength range of 400-760 nm. So, we can get a minimum resolution of about 200 nm. However, in the SEM, the electron wavelength is much smaller, so the minimum resolution of a SEM can be about 3-6 nm.

Figure 10. A scanning electron microscope SU70 SEM picture at the USF NREC. [Adopted from SU70 SEM, by Jay Bieber, 2019 (http://www.nrec.usf.edu/documents/tools/Hitachi%20SU70%20Scanning%20Electron%20Microscope.pdf)]

Under the action of an accelerating voltage, the electron beam emitted by the electron gun will converge through a magnetic lens system to form an electron beam and focus on the sample surface. Under the action of the deflection coil between the condenser and the objective lens, the electron beam scanned on the sample, and the electrons interact with the sample to generate electronic signals. The detector collects these signal electrons and converts them into photons, which are further amplified and processed by an electrical signal amplifier. Finally, an image projected on the display screen.

4.3 EDS (Energy Dispersive Spectroscopy)

The elemental analysis of both commercial dyes based, and blue dye samples are characterized by energy dispersive spectroscopy. The EDS analytical working distance is 10 mm with a take-off angle of 60°and the accelerate voltage is 15 kV. The number and energy of the X-rays emitted from a specimen can be measured by an energy-dispersive spectrometer. As the energies of the X-rays are characteristic of the difference in energy between the two shells and of the atomic structure of the emitting element, EDS allows the elemental composition of the specimen to be measured in terms of either atomic percentage and/or weight percentage.

4.4 TEM (Transmission Electron Microscopy)

Transmission electron microscopy (TEM) is similar as scanning electron microscopy. Both SEM and TEM use electrons as a probe to maximize the resolution while TEM (Figure 11) has a higher acceleration voltage (50 kV to 500 kV). To prepare a sample for TEM analyzing takes a long time (1 hour) because the sample should be thin enough (less than 100 nm) so that electrons can transmit through to form an image. When electrons transmit through the specimen, the interaction between the beam and the specimen will generate several signals that can be detected by different detectors. They are the interface between our eyes and electrons when we cannot see electrons directly. Like Cathodoluminescence (CL) can convert the energy of the electrons (cathode rays) to produce light (luminescence).

A transmission electron microscope is the key instrument to determine if the encapsulation is successful or not because it can offer a higher resolution to allow the delineation of the sample's surface morphology.

20
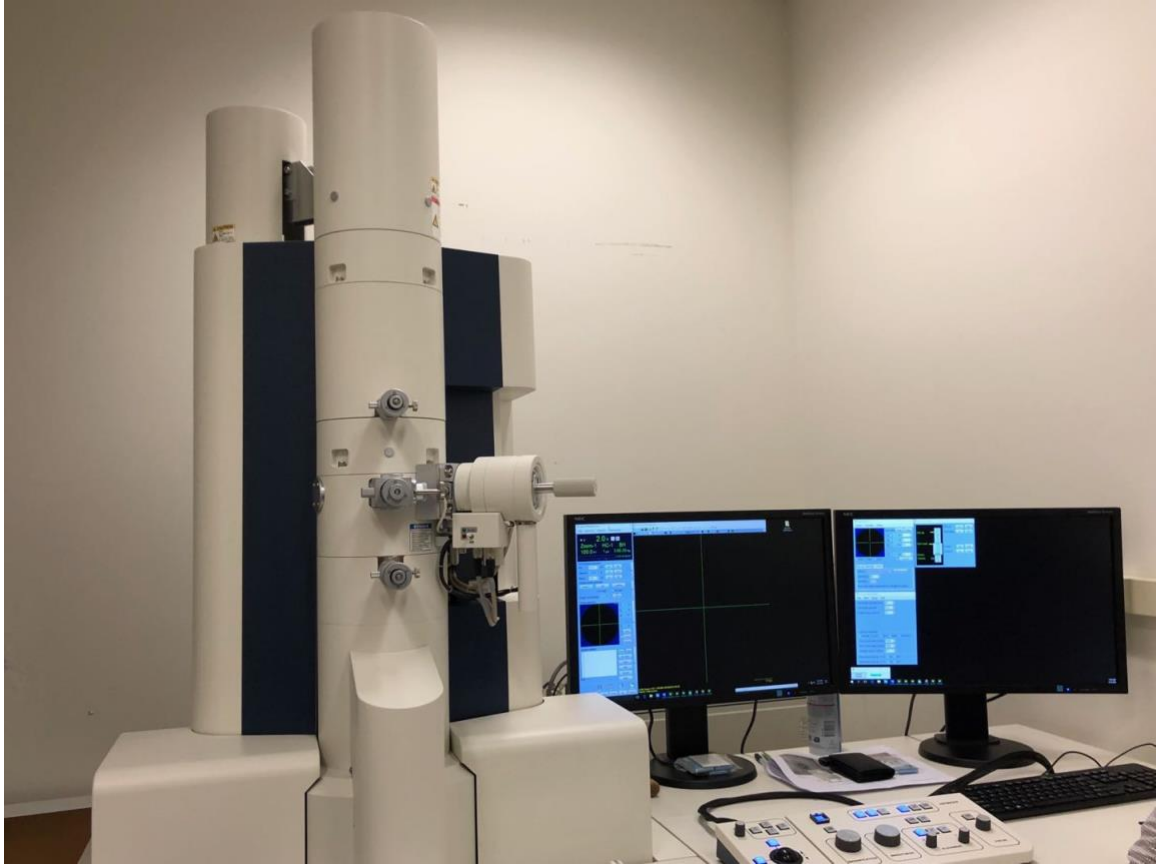
Figure 11. Picture of the TEM HT7800series at the UF

4.5 TGA (Thermogravimetric Analyzer)

The thermogravimetric analyzer is a thermal analysis method to understand the thermal stability by measuring the mass loss as a function of temperature as the temperature increases over a specified range. If the mass of the TC material stays the same in a specific temperature range, then the material is stable and keeps its functionality over that temperature range. The TC material can be considered to degrade when at a certain temperature it begins to change its mass. It seems important to determine the stable range since TC material is encapsulated with a polymer and the melting point of the co-solvent is low. Additional conclusions can be reached from the results of three basic measurements: time, mass and temperature, considering oxidation and combustion.

21

4.6 DLS (Dynamic Light Scattering)

Dynamic Light Scattering (DLS) was carried out on different samples at different temperature to see the particle size difference due to encapsulation and temperature. Dynamic light scattering is a technique because particles scatter light of a wavelength, such as Helium-Neon laser at $\lambda = 632.8$ nm. During the testing, the scattering volume is constant, and the particles diffuse out of this volume over time. In Equation (7), it shows the Stokes-Einstein Debye relation that given the relation between hydrodynamic volume, viscosity, temperature and the Boltzmann constant.

$$d(H) = kT / 3\pi\eta D \quad (7)$$

(where D is translational diffusion coefficient, $d(H)$ is hydrodynamic diameter, T is the absolute temperature and η is the viscosity, k is Boltzmann's constant.)

The instrument will avenge all results after 120 times testing in total to form a more relievable results.

4.7 DSC (Differential Scanning Calorimetry)

Differential Scanning Calorimetry is a technique to analyze the thermol property of material such as its melting point and enthalpy requirement. It needs to meansure both sample and reference material for each experiment. Usually, the temperature program for DSC is designed to draw a figure such the sample temperature increases linearly as a function of time. It contains exo and endo process which means release heat and absorb heat during the test. For thermochromic material, we run dsc for both plain dye and encapsulated dye to see how the encapsulation influence the enthaoy of the sample also to make sure the encapsulation condition.

22

Chapter 5: Results and Discussion for TCM at SiO_2

5.1 Results and Discussion

This chapter presents the significant results obtained from different characterization techniques for both the original dye and the encapsulated dye to obtain a better understanding of the encapsulation process. Each of the equipment, SEM, EDS, TEM, DSC, and TGA can provide unique information on to the sample properties, when the original dye is used as a reference. For all the samples made from the commercial dye, powder samples were obtained after filtration and thermal treatment.

5.2 Thermochromic Properties

Tables 1 and 2 contain all the design of experiments carried out in the encapsulation process but with different parameters. In all the experiments, a thermal plate was used to heat each sample to see if it shows the thermochromic (color change) property. Samples showing color change are stored for further tests. Some samples that did not show color change around 30º C were not characterized but kept for future research. The blue dyes consisting of CVL, Bisphenol A and 1-tetradecanol are liquid during the encapsulation process, due to the high temperature (70ºC), and become solid after encapsulation when the temperature cooled down to room temperature. Base on this phenomenon, emulsion end samples may not have been fully encapsulated and, therefore, not suitable for characterization.

Color change of Black dye.

Table 1. Design of experiments with different surfactants

Sample #	Solvent	Surfactant	Dye	Precursor	Catalysts	Color change point	Final solution
S1	DI water 80ml	SDBS 1g	black dye 0.5g	TEOS 3ml	Ammonia 2ml	31 °C	suspension
S2	DI water 80ml	Poly (sodium 4-styrenesulfonat) 1g	black dye 0.5g	TEOS 3ml	Ammonia 2ml	31 °C	suspension

Samples 1 and 2 have different surfactant and yet both change color at 31°C. However, the SEM images show sample 2 having a non-uniform particle formation in the microscale. From samples 3 to 6, all experiments ended with an emulsion form. which means the concentration difference of the dye did not cause failure of encapsulation. In addition, samples 6 and 7 indicate that the surfactant has not caused the encapsulation failure. Therefore, the new experimental process carried out in chapter 3 could yield a suspension form. Adjustments, including the order of adding chemicals and reaction time may be necessary.

Table 2. Design of experiments. Different dye concentrations (sample 3-7) and different surfactants (sample 6 and 7) and new experiment sample 8.

Sample #	Solvent	Surfactant	Dye	Precursor	Catalysts	Color change point	Final solution
S3	DI water 80ml	SDBS 1g	Blue dye 2.7ml	TEOS 3ml	Ammonia 2ml	31 °C	Emulsion
S4	DI water 80ml	SDBS 1g	Blue dye 5.4ml	TEOS 3ml	Ammonia 2ml	31 °C	Emulsion
S5	DI water 80ml	SDBS 1g	Blue dye 8.2 ml	TEOS 3ml	Ammonia 2ml	31 °C	Emulsion
S6	DI water 80ml	SDBS 1g	Blue dye 20ml	TEOS 3ml	Ammonia 2ml	31 °C	Emulsion
S7	DI water 80ml	CTAB 1g	blue dye 20ml	TEOS 3ml	Ammonia 2ml	31 °C	Emulsion
S8	DI water 80ml	SDBS 1g	Blue dye 10ml	TEOS 3ml	Ammonia 2ml	31 °C	Suspension

24

In addition, some pictures are taken to show the color change of BDTCM at SiO$_2$. The BDTCM at SiO2 are change color form blue to white when temperature go through from 25 to 35. And they are shown in following figure 12.
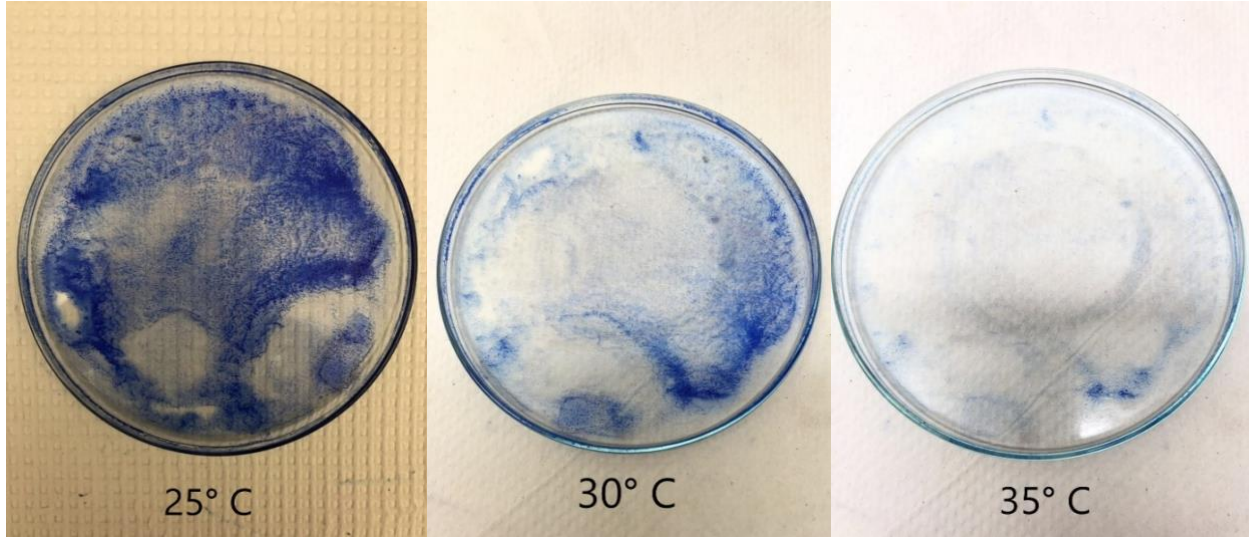
Figure 12. Color change of BDTCM at SiO$_2$ at different temperature

5.3 Micromorphology and Elemental Analysis Using the SEM-EDS

5.3.1 Micromorphology and Elemental Analysis via SEM-EDS for CDTCM at SiO$_2$

The morphology and elemental composition analysis of all samples are done by using scanning electron microscopy (SEM) simultaneously with energy dispersion spectroscopy (EDS). The powder sample, finely ground, was set up on the holder first for gold sputtering to eliminate any charge effect during SEM running. For the CDTCM at SiO$_2$ sample, the image captured by the SEM (Figure 13) shows that morphology of the TCM at SiO$_2$ particles is clearly spherical with size ranging from 100 to 1000 nm.
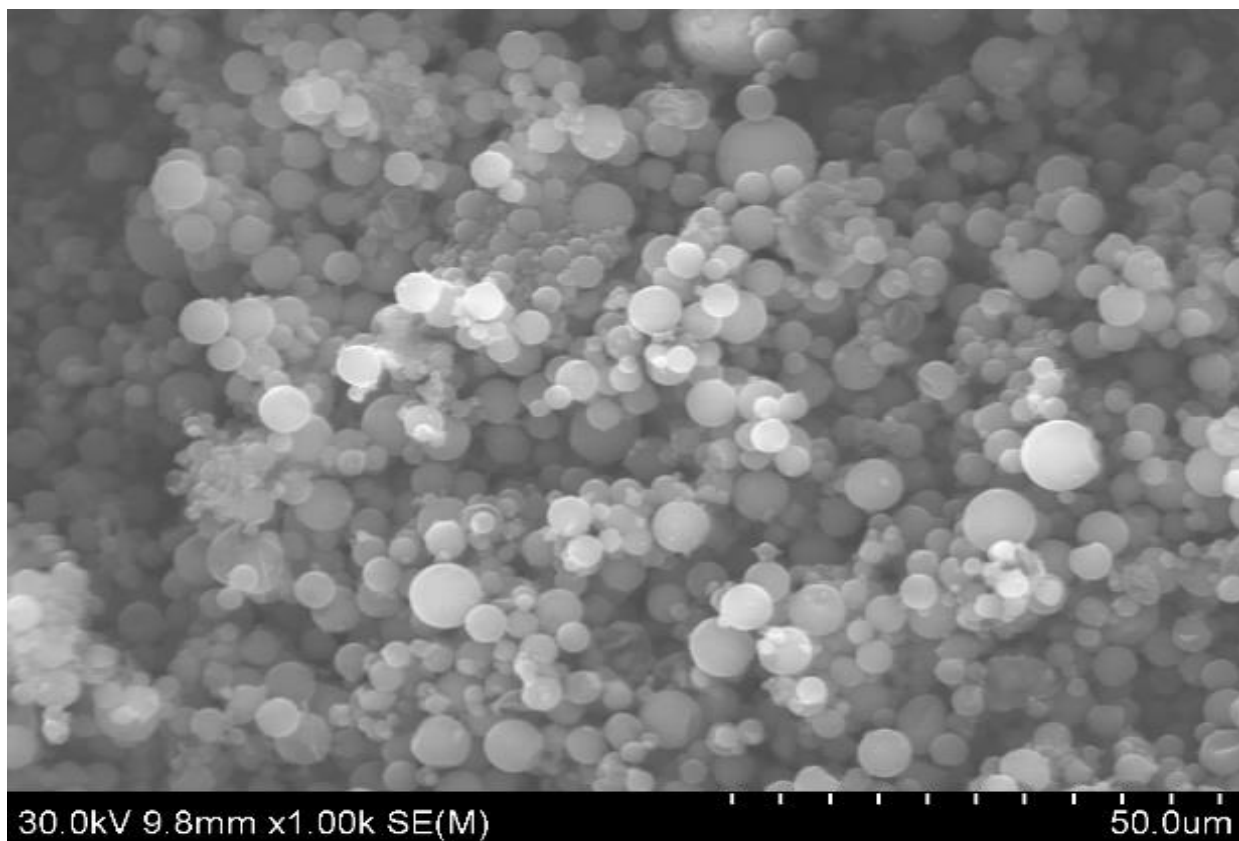
Figure 13. SEM image of CDTCM at SiO$_2$ particles.

From the EDS results, Table 3 shows all of the elements present in the commercial dye including carbon, oxygen, sodium, and chlorine. It is easy to see that carbon and oxygen are the main components because the dye is organic and is coated with a polymer. Trace amounts of sodium and chlorine may originate from the dye or contamination, because it was purchased from a company and not further purified.

Table 3. EDS results for the commercial dye.

Elt.	Line	Intensity (c/s)	Error 2-sig	Low KeV	High KeV	Atomic%	Conc	Units
C	kα	3,298.43	15.290	0.220	0.334	81.776	76.752	Wt%
O	kα	286	4.907	0.471	0.579	17.741	22.189	Wt%
Na	kα	26.86	2.794	0.983	1.099	0.319	0.574	Wt%
Cl	kα	21.13	2.666	2.553	2.692	0.164	0.455	Wt%
						100.00	100.00	Wt% total

26

In Table 4, we can assume that silicon is present in the CDTCM at SiO₂ sample with a concentration of about 0.4 wt%, and oxygen concentration of about 2.3 wt%. The percentage of Si is not high enough because the condensation of the precursor took place at a slower rate than expected. Aluminum is not supposed to be present, and it could be due to contamination from the aluminum foil that covered the sample or the Al sample holder.

Table 4. EDS result for CDTCM at SiO₂

Elt.	Line	Intensity (c/s)	Error 2-sig	Low KeV	High KeV	Atomic%	Conc	Units
C	Kα	3,134.26	14.958	0.220	0.334	79.979	74.754	Wt%
O	Kα	315.47	5.111	0.471	0.579	19.669	24.490	Wt%
Al	Kα	19.15	2.904	1.425	1.548	0.163	0.342	Wt%
Si	Kα	23.42	3.002	1.677	1.803	0.190	0.414	Wt%
						100.00	100.00	Wt% total

Based on just the EDS results in Figure 14, we can assume that SiO₂ is formed from the TEOS precursor because the original precursor and the intermediates are dissolvable in 10% ethanol and could be removed during the sample wash step. But we cannot make conclusion that dye material are encapsulated which means silicon dioxide is in sample but its encapsulated or it form particles itself is not clear. It means further characterization are nesseersory as well. Moreover, some parameters may need to be adjusted to accelerate the condensation process to increase the final SiO₂ concentration. Also, using different techniques to storage samples need be used to eliminate cross-contamination. Like using lab films to cover samples and glass tube to storage.
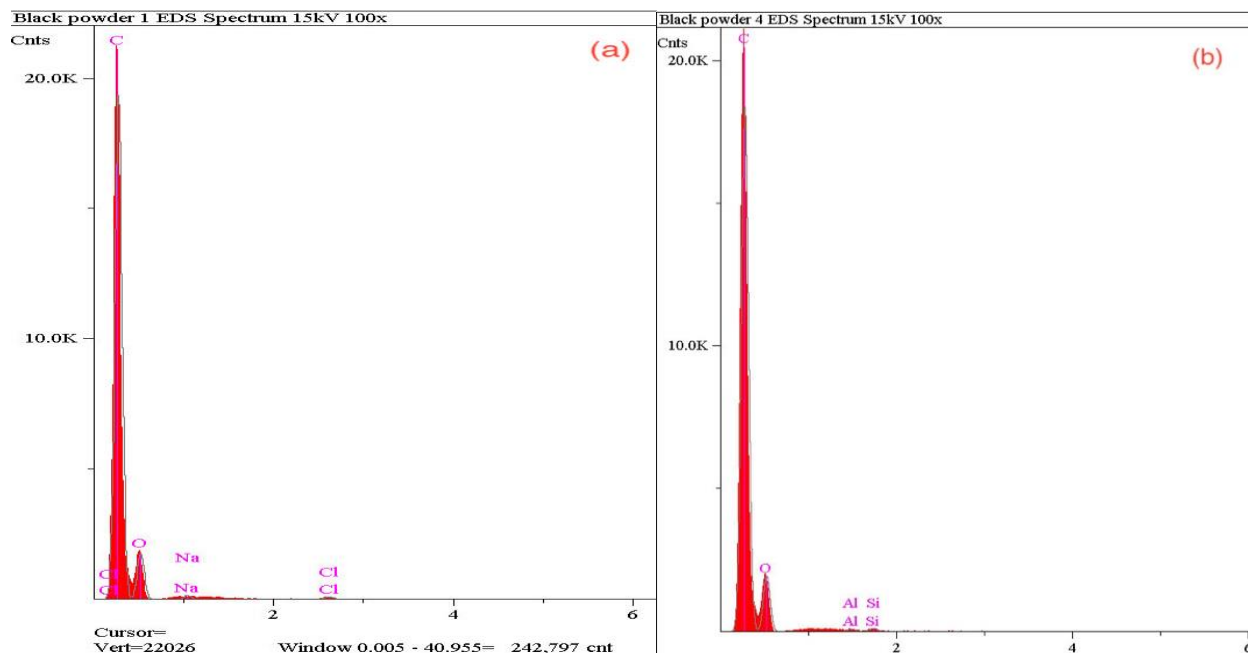
Figure 14. EDS results for (a) commercial dye; and (b) CDTCM at SiO_2

5.3.2 Micromorphology and Elemental Analysis via SEM-EDS for BDTCM at SiO_2

For the blue dye thermochromic material encapsulated with SiO_2 (BDTCM at SiO_2), the solution settled at the bottom of the glass flask, while the sample was centrifuged with following low temperature (50 °C for 24 hours) drying process, was used for the SEM testing. Figure 15 shows the SEM results obtained from backscatter electron model. Even though they are not uniform, we can detect small white particles are embed into continuous organic substrate. From this SEM images, we cannot give the conclusion that blue dye is encapsulated or not, but we can state that its micro structure including two different form: small particles and continuous bulk. if we consider the bulk is the organic Blue, then the particle may refer to encapsulated blue dye. But we cannot ensure that just based on the SEM images. Also, since the charge effect, it is difficult to go higher magnification to ensure the particle size and surface morphology, and that is why TEM are used and analyzed in next section to have a better understanding of particle morphology.

28
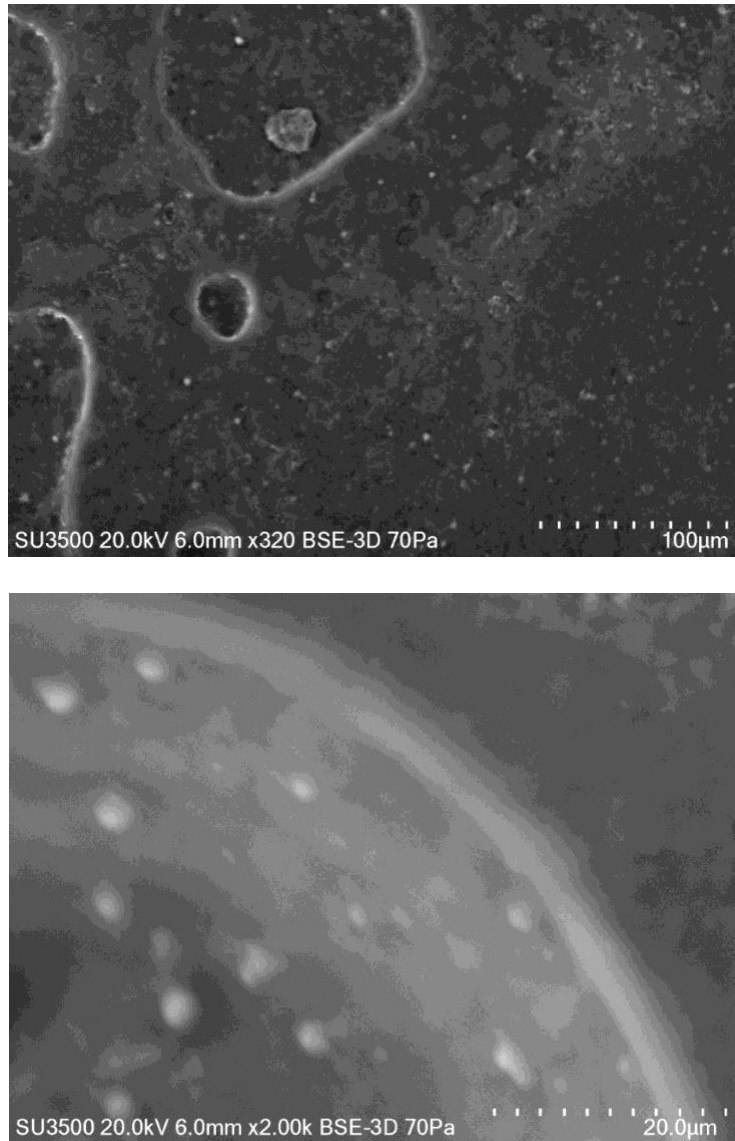
Figure 15. SEM BSE images of BDTCM at SiO_2

To ensure the composition of BDTCM at SiO_2, EDS elemental analysis and EDS mapping were applied, and the results are shown in Table 5 and Fig. 16. Based on Table 5, the concentration of carbon, oxygen, sodium, sulphur, and silicon are 66.95%, 20.22%, 1.77%, 2.35%, and 1.62% separately. The weight pasentage of titianium, iron, siliver and calcium are too low that can be exclude from the sample. Carbon, which is the main element ocupide 66 wt% is from the organic blue dye. Oxegen is second main element which is come from both organic blue dye and silicon dioxide. Mean while, Sodium is attributed by SDBS that we used as

29

surfactant. The pesantage of silicon is 3.38 wt% which is not high as we expected but it shows

that SiO_2 is exit in the sample and comes from purcusor TEOS. The condensation of TEOS

should be faster to increase the silicon concentration to form more encapsulatied particles. More

mapping images are attached in the end of this thesis as appendix A.

Table 5. EDS result for BDTCM at SiO_2

Element	Line Type	Apparent Concentration	k Ratio	Wt%	Wt% Sigma	Standard Label
C	K series	9.27	0.09272	66.95	0.17	C Vit
O	K series	3.43	0.01153	20.22	0.17	SiO2
Na	K series	1.77	0.00746	4.12	0.03	Albite
Si	K series	1.62	0.01287	3.38	0.02	SiO2
P	K series	0.19	0.00105	0.27	0.01	GaP
S	K series	2.35	0.02028	4.71	0.03	FeS2
Ca	K series	0.11	0.00098	0.21	0.01	Wollastonite
Ti	K series	0.00	0.00003	0.01	0.01	Ti
Fe	K series	0.05	0.00051	0.12	0.01	Fe
Ag	L series	0.01	0.00006	0.01	0.02	Ag
Total:				100.00		
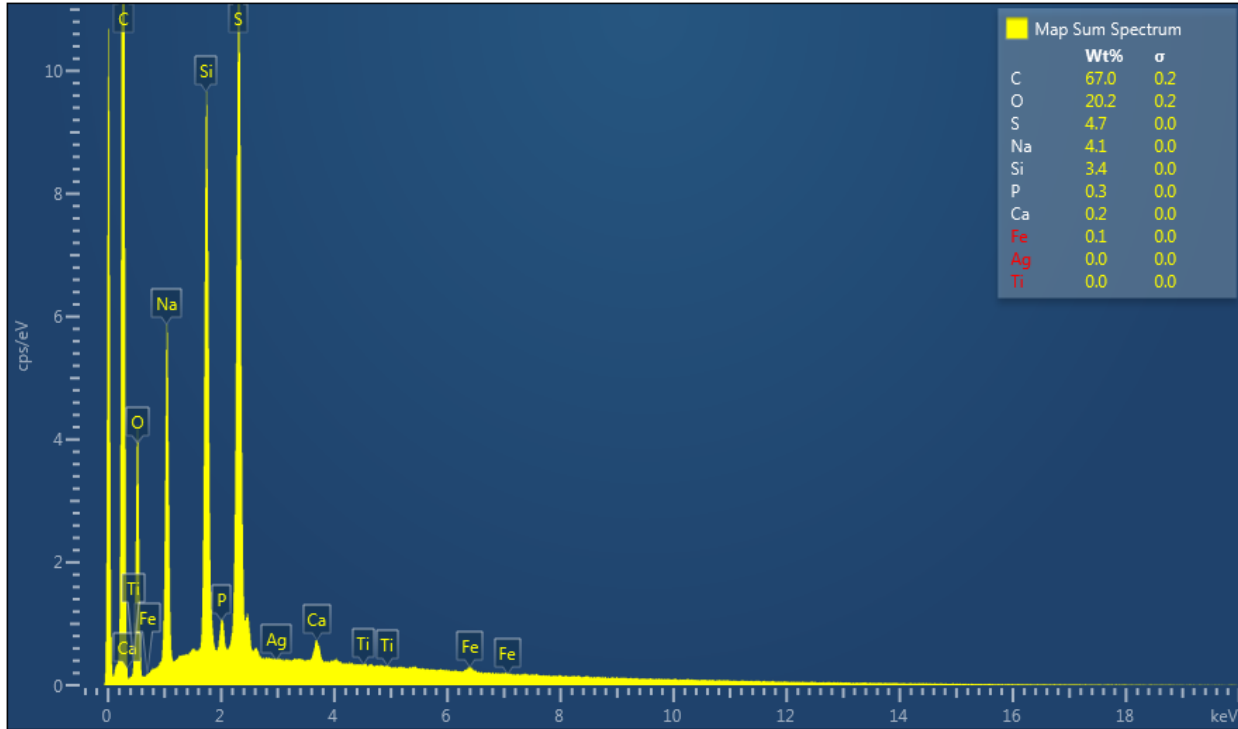
Figure 16. EDS mapping of the BDTCM at SiO₂ sample.

5.4 Microstructure and Surface Morphology using TEM

5.4.1 Microstructure and Surface Morphology of CDTCM at SiO₂ via TEM

The powder samples are first dissolved in ethanol to reduce the concentration and achieve the TEM requirements. By using TEM, we ensure the particles are uniform and spherical, which was the conclusion from the SEM results. Additional information is obtained using the TEM, such as surface morphology. Figure 17 (a and b) shows with the same resolution TEM images of two specific particles of the commercial dye encapsulated with silicon dioxide.
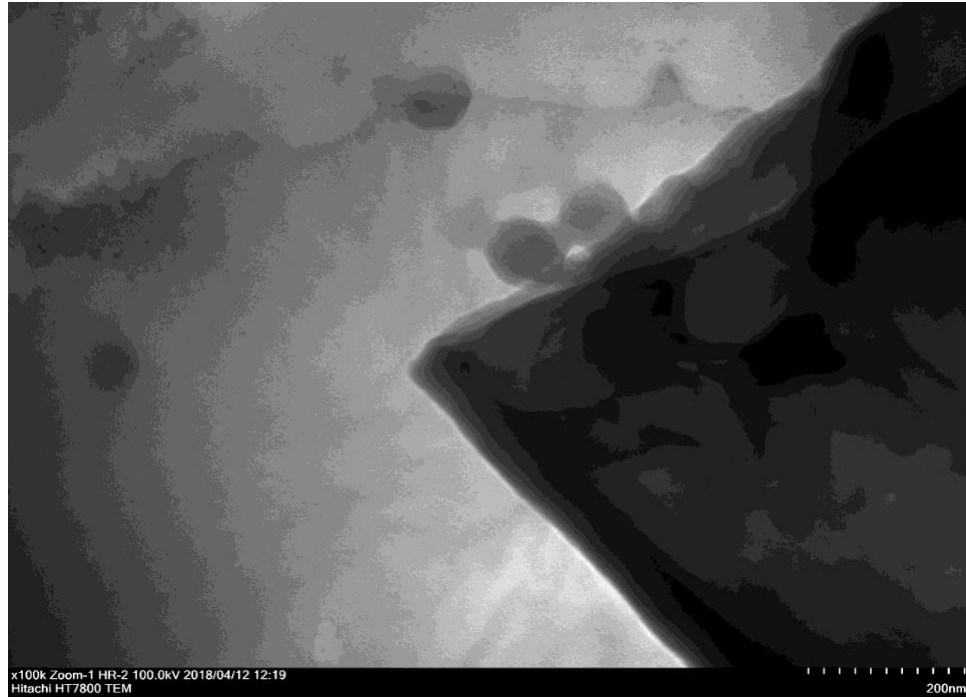
(a)

(b)

Figure 17. TEM images of the CDTCM at SiO_2

Since the original particles were coated with a polymer, it is hard to define the shell

material, but we can just confirm its core-shell structure. By using the higher resolution of TEM,

one can compare the particles (a) and (b). The surface of particle (a) is much flatter than that of

32

particle (b) which implies different surface structures. It is obvious that the particle (b) has greater number of small particles on its surfaces, which can consider to be silicon dioxide, and particle (a) can be considered as the original surface of the commercial dye. Why particle (a) does not have greater amount of silicon dioxide is probably because the concentration of SiO_2 is low (0.41wt%), as previously shown in the EDS results.

Combining the SEM and TEM results, we can conclude that the encapsulation process is successful and that silicon dioxide particles are adsorbed on the surface of the commercial dye together with the existing polymer. To improve the percent of encapsulation, higher concentrations of the silicon dioxide precursor (TEOS) or the catalyst (ammonia) are needed.

5.4.2 Microstructure and Surface Morphology of BDTCM at SiO_2 via TEM

For the blue dye, the core and shell are made separately, then they are dissolved in acetonitrile first to prepare the sample holder for TEM testing. During the sample preparation, the BDTCM at SiO_2 powder did not dissolve in ethanol and this was unexpected. The reason is the silicon dioxide shell is not dissolvable in ethanol.

Figure18 shows the microstructure of BDTCM at SiO_2 and figuer 19 shows its surface morphology. Figure 17 shows that the average particle size of the BDTCM at Si_{O2} is much smaller than that of the CDTCM at SiO_2 because the BDTCM at SiO_2 is encapsulated without polymer.
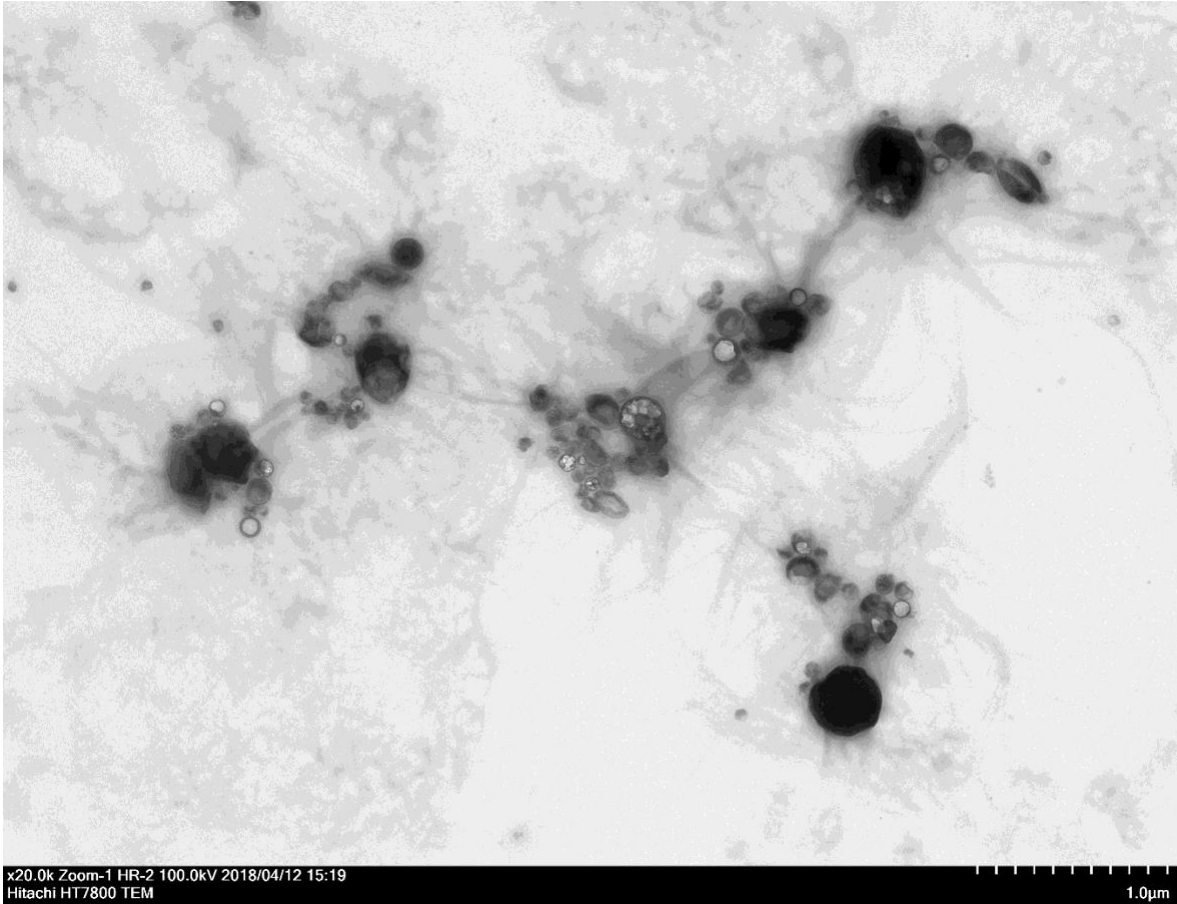
Figure 18. Microstructure of BDTCM at SiO_2

We can also see the particle size has a various range because it is significantly influenced by the stirring speed and surfactant concentration, which was mentioned in Xiaoye Geng's paper [45]. When a specific particle is magnified, as shown in Figure 18, one can see two types of encapsulated particles, (a) and (b), both showing a perfect spherical structure. In particle (a), we can see its diameter being less than 100 nm and its core-shell structure with many small particles around its center. Particle (b) shows a smoother and more uniform ring which may be considered as better encapsulation. This could also be the result of surfactant concentration and stirring speed.

34
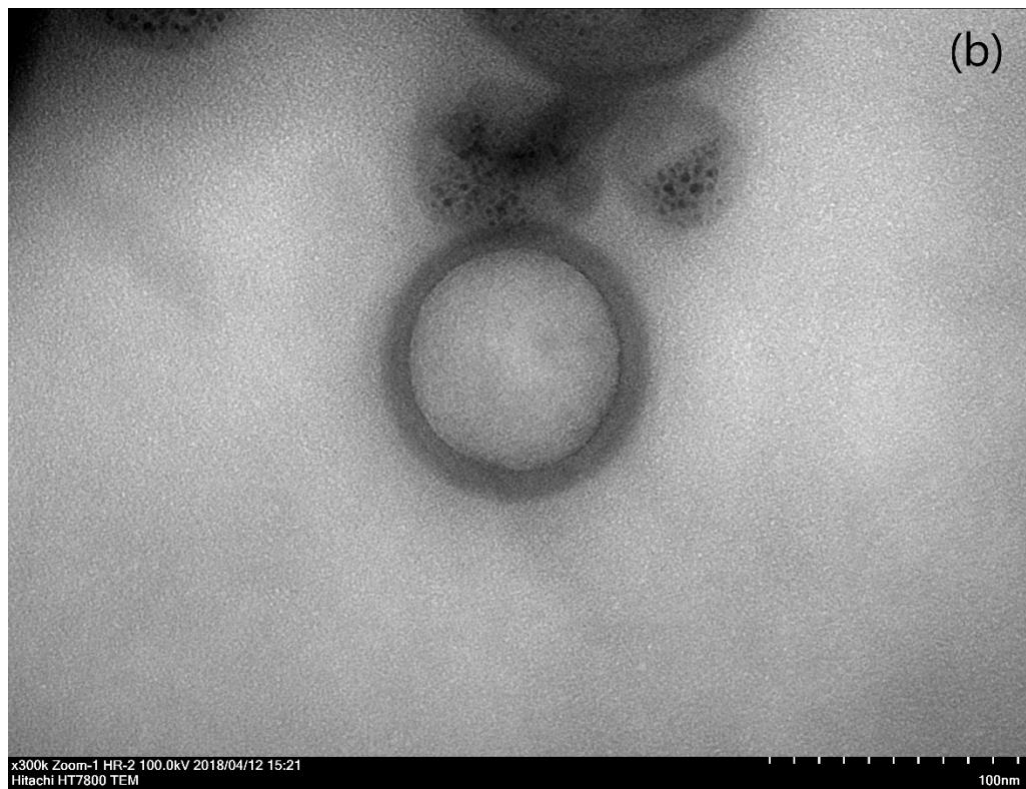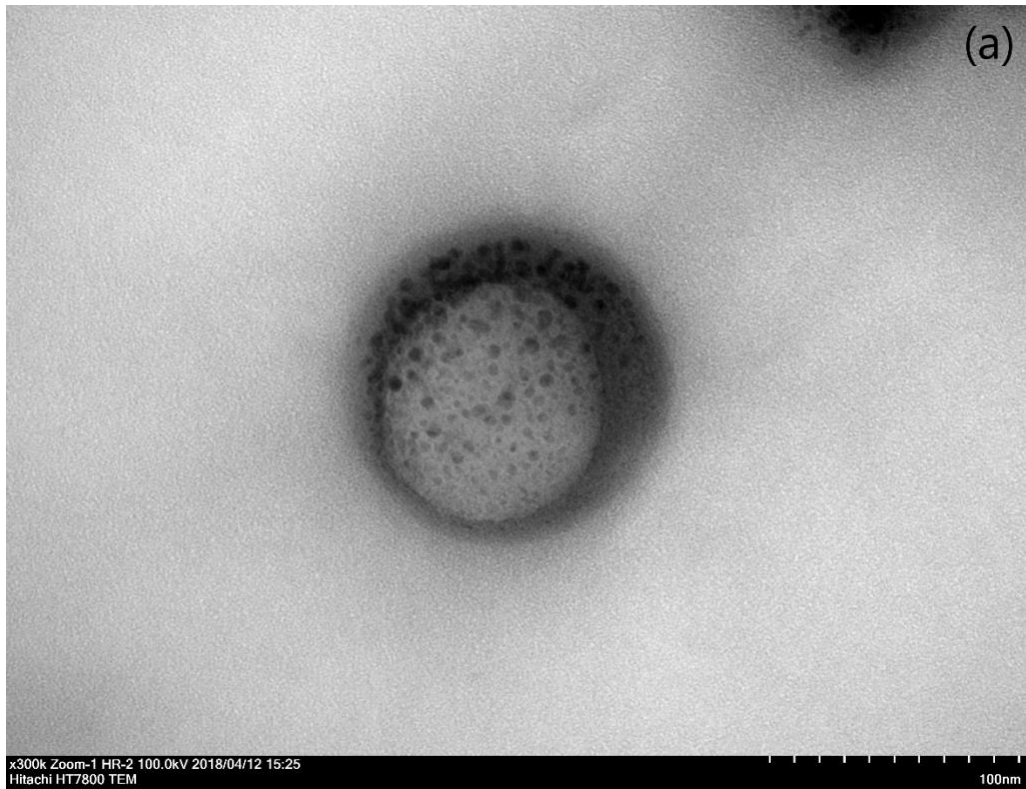
Figure 19. TEM images of the BDTCM at SiO_2

5.5 Particle Size Analysis by Dynamic Light Scattering (DLS)

The DLS test provides information for the average particle size and particle size range in a sample which could then be related to the encapsulation state of the dye. The final result is the avenge of 36 results from 36 texting which means running thirteen times for each round and three rounds in total. For each sample, different temperature, 20ºC, 30ºC and 40ºC are applied to investigate the temperature influence for particle size. All samples are consisted of 20 micrograms dissolved in 1 ml of DI water and mixed by ultrasonic vibration for 2 minutes. Two minutes that it reached the set temperature, the temperature of the tube that contains the sample. The results were then extracted from the DLS software particle size distribution report as shown in Table 6 for the commercial and blue dye samples. Detailed reports of each texting are shown in the appendix.

Table 6. Particle size of commercial dye, CDTCM at SiO_2 and BDTCM at SiO_2

Particle size (nm)	20º C	30º C	40º C
Commercial dye	2186	2014	1896
CDTCM at SiO_2	2443	2665	2445
BDTCM at SiO_2	285.7	429.6	403

For the commercial dye, larger particle sizes obtained at 20º C is due to its agglomerative nature, however, the particles disintegrated and hence the lower particle sizes in the order of 30º C and 40º C. Moreover, at around 30º C, color changes occur where the particle size reduction is plausible. Commercial dye with SiO_2 shows increasing particle sizes when compared to commercial dye. This may be due to the thin encapsulating layer of SiO_2 (this is the reason why the TGA curves are very similar for both encapsulated and plain dye samples discussed in section 5.7) to cover TC material thus enhances the overall particle sizes. During the color

36

change region of 30° C, even the powder gets agglomerated, however after such color change, at

40° C, it becomes the same particle size as similar as 20° C.

5.6 Thermal Property Analysis via Differential Scanning Calorimetry (DSC)

5.6.1 Thermal Property Analysis by DSC

The powder sample for the DSC is loaded directly in the instrument and the parameters

obtained are as shown in Table 7. About 5 mg size samples are suitable for DSC testing at

temperature ramp rate of 5° C per minute to allow greater detail near the critical point (color

change point). The range is set from 0 to 60° C to save testing time and energy, because we know

the critical point is about 31° C. The cool down process is set at the same ramp rate with the

results also recorded. Both results, for the commercial dye and the CDTCM at SiO$_2$ are plotted

and shown in Figure 20, with the data being collected and organized as shown in Table 8.

Table 7. Testing parameters for the, commercial dye and the CDTCM at SiO$_2$

Sample name	Sample mass	T ramp rate	Start T	End T
Commercial dye	4.3 mg	5° C/min	0° C	60° C
CDTCM at SiO$_2$	5 mg	5° C/min	0° C	60° C

Table 8. DSC results of commercial dye and sample CDTCM at SiO$_2$.

Samples	Endothermic peak temperatures (Heating) (° C)	Exothermic peak temperatures (cooling) (° C)	Enthalpy (heating | cooling)(J/g)
Commercial	33.03| ~29.72	26.4 | 23 | 14.6	95.021 | 87.442
CDTCM at SiO2	~32.6 | 29.72	26.4 | 22.5	97.558 | 91.749
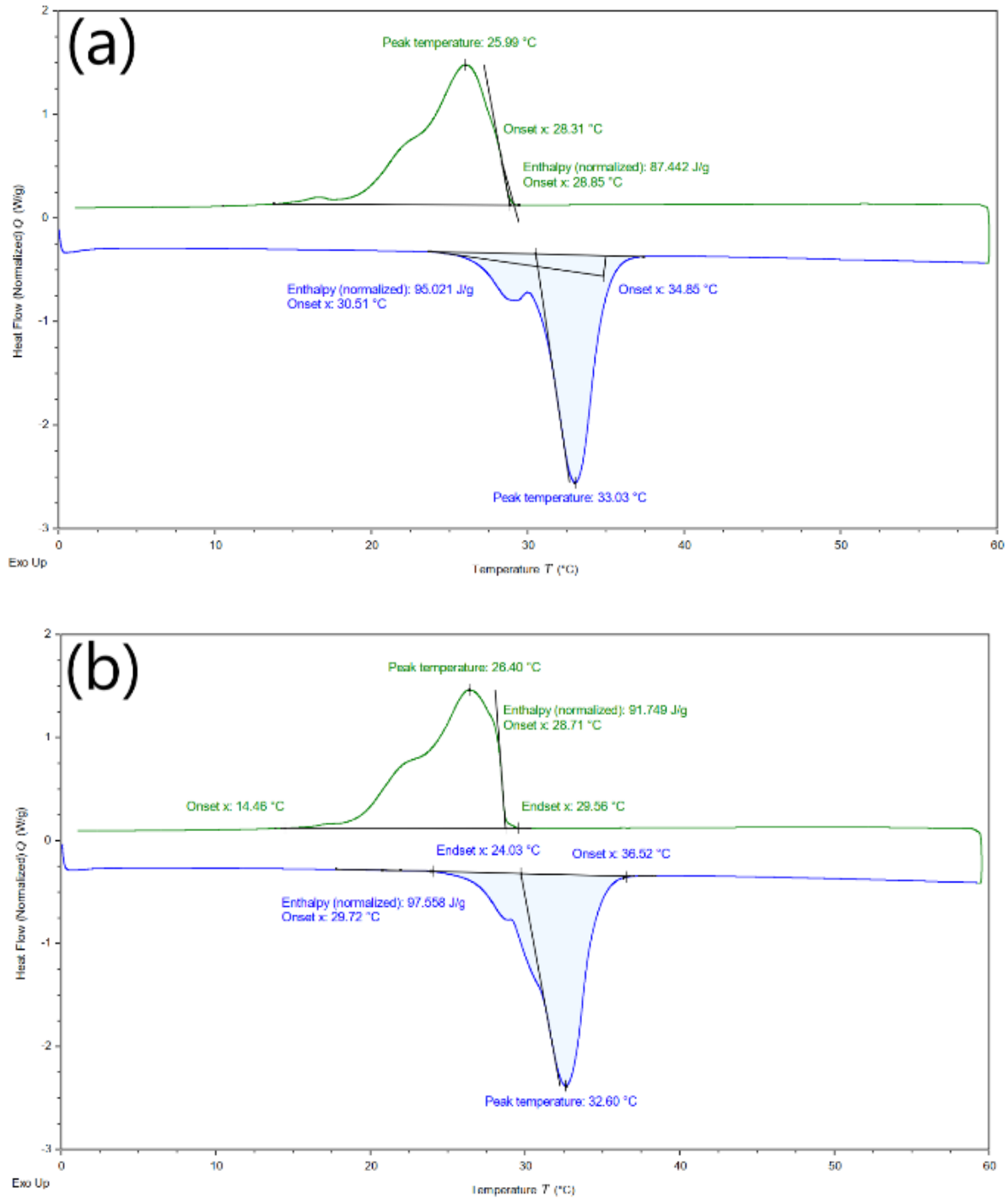
Figure 20. DSC results for the (a) commercial dye and the (b) CDTCM at SiO$_2$.

For the commercial dye, one sees over layered two peaks, one small and one big, at the end of the process, which possibly is because of the two different organic crystal morphologies.

It could also suggest that the commercial dye may contain an irregular nucleated structure and sphere structure where all the crystallites are roughly symmetric. So, either one of these is not a perfect crystal structure with a lot of defects that means it is going to melt more easily and show up as the lower melting peak. In contrast, the other structure is highly ordered and close to perfect, that means they will melt at a higher temperature and will show as the peak at a higher temperature.

5.7 Thermal Stability via Thermogravimetric Analysis (TGA)

5.7.1 Thermal Stability of Commercial Dye and CDTCM at SiO2 via TGA

Samples for the TGA test were about 3-4 mg for both the commercial dye and the CDTCM at SiO_2. The temperature range was set from room temperature (25° C) to 600° C with a ramp rate of 10 ^{o}C per minute. The nitrogen flow rate was set at 5 0ml per min during the entire testing process. The results are organized in Table 9 to show the detail of the two significant weight loss steps. The TGA results are also plotted and shown in Figure 21.

Table 9. TGA results for the commercial dye and the CDTCM at SiO_2

Sample	Step one T (onset | end set)	Step one loss (weight | %)	Step two T (onset | end set)	Step two loss (weight | %)
Commercial dye	206° C | 324° C	0.3627mg | 10.10%	330° C | 496° C	2.6544mg | 73.94%
CDTCM at SiO_2	226° C | 322° C	0.2522mg | 8.40%	328° C | 496° C	2.0638mg | 68.77%

39
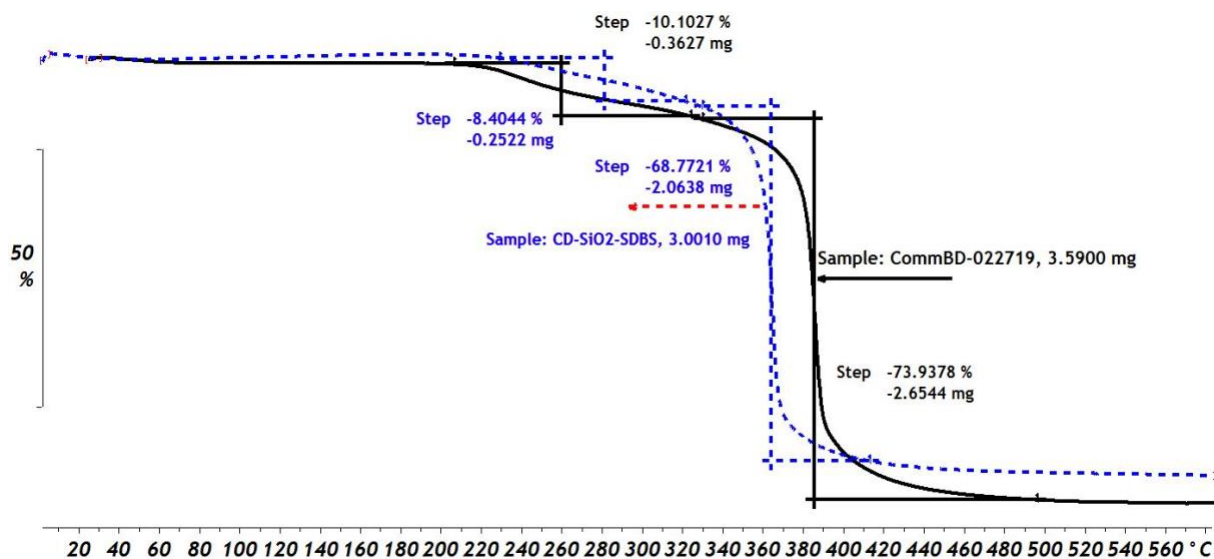
Figure 21. DSC results for the commercial dye and the CDTCM at SiO2

The first weight reduction step is due to polymer weight loss and the second due to the

dye weight loss. It is noticeable that the weight loss of CDTCM at SiO2 is less than the

commercial dye, which means the SiO2 shell on the polymer surface may store some energy that

retards the polymer degradation. Furthermore, the CDTCM at SiO2 starts losing weight 20° C

higher than the commercial dye, which also confirms that the SiO2 shell could store high latent

heat. For step two, CDTCM at SiO2 also shows less weight reduction (5.2%) which may benefit

from the protection of SiO2 shell. The reason why the protection is not significant is the low

concentration of SiO2 which just partially encapsulated on the dye surface.

5.7.2 Thermal Stability of Blue Dye and BDTCM at SiO2 using TGA

Blue dye samples for the TGA test were 3.5 mg and 5.3730 mg for the CDTCM at SiO2.

The temperature range was set from room temperature (25° C) to 600° C with a ramp rate of 10

°C per minute. The nitrogen flow rate was set at 50ml per min during the entire testing process.

The results are organized in Table 10 to show the detail of the two significant weight loss steps.

The TGA results are also plotted and shown in Figure 22.

40

Table 10. TGA results for the plain blue dye and the BDTCM at SiO_2

Sample	Step one T (onset | end set)	Step one loss (weight | %)	Step two T (onset | end set)	Step two loss (weight | %)
Blue dye	100º C | 225 ºC	3.4478mg | 98.51%	NA	NA
BDTCM at SiO_2	100º C | 225 ºC	4.0724mg | 75.79%	400º C | 485º C	0.4041mg | 7.52%
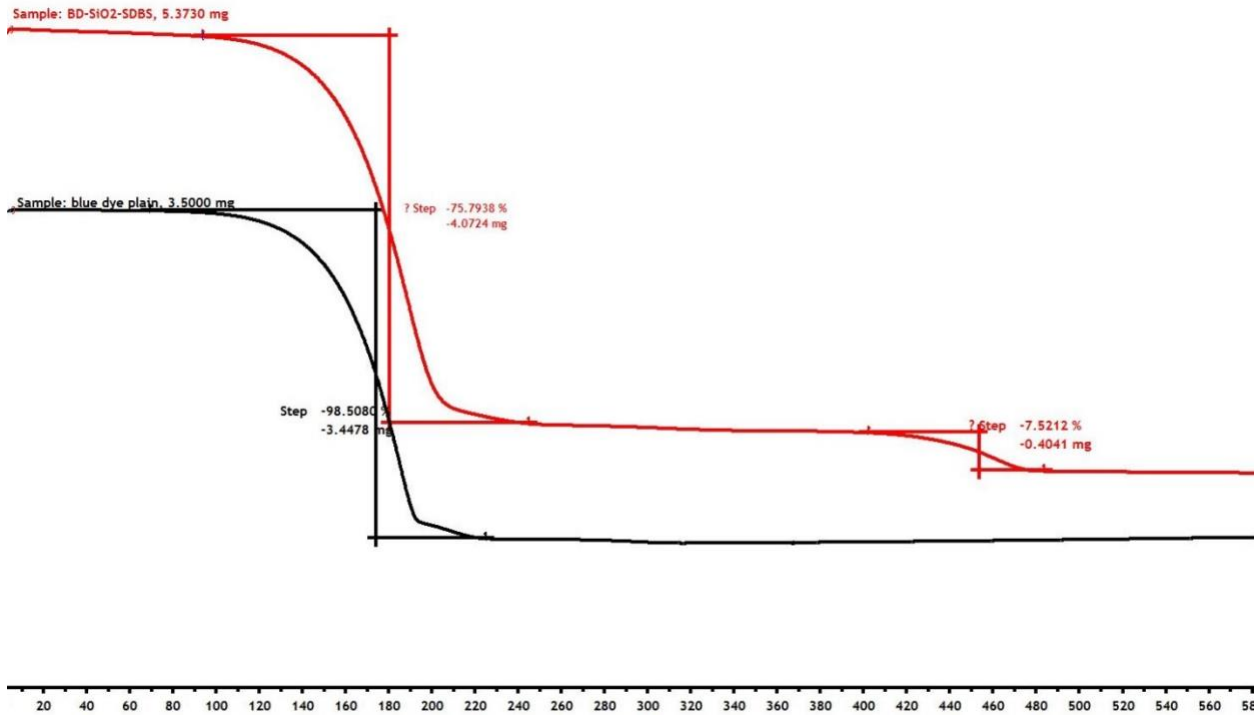
Figure 22. DSC results for the commercial dye and the CDTCM at SiO2

The TG curve of Blue dye had two degradation steps in Figure 22(black color). The onset temperature is about 100º C, which was attributed to the decomposition of tetradecanol, the following weight reduction from 190 to 225º C is considered as the decomposition of BPA and CVL [47]. Therefore, the blue dye degrades about 98% in total. Meanwhile, the thermal stabilities of CDTCM at SiO_2 was also analyzed by TGA experiments. As shown in Figure 22(red color), a similar weight loss (75.79%) occurs from 100 to 225º C which is the dye decomposition. And a 7.5212% weight loss from 400 to 485º C is the decomposition of silica-bonded groups such as -OH group [47]. And the final residual weight is 16.68%. for the first

41

step, the weight loss of BDTCM at SiO2 is 22.8% less than plain blue dye. If we combine the results from SEM, we know the Si weight percentage is 3.4% and for SiO_2 is about 7.28%. therefore, weight residual cannot all be the SiO2 because 16.68% is 9.4% bigger than 7.28%. one reason can be that the weight remain is both blue dye and SiO2 and Blue dye is inside the SiO_2, so it did not degrade at the first step.

Chapter 6: Conclusions and Future Works

Based on the results obtained using different characterization tools, the encapsulation process is successful complete by *in-situ* encapsulation mothed. It is the first time to create a SiO_2 coated commercial dye. It is meaningful because the method can be applied to any other metal oxide encapsulation, which could give the thermochromic material multi-properties. In this thesis, the encapsulation is not just success on the commercial dye, but also blue dye (three component system). They have different application because they have a different color change which commercial dye is from black to white and blue dye is from blue to white while temperature changes. Results of DSC may also indicate encapsulated thermochromic material could be a thermal energy storage material due to large enthalpy values.

Even the encapsulation is completed, but it still needs to be developed due to some testing results. Precursor concentration may need to be adjusted to form a thicker layer of silicon dioxide because the EDS show the SiO_2 percentage is not high enough. Also, some parameter like stirring speed and emulsifier concentration need to be investigated to form a more uniform structure for BDTCM at SiO_2. Furthermore, we should start investing its scalability for commercial application. Studying its energy and money cost, and environmental substainability.

43

References

1. Kulčar, R., Friškovec, M., Hauptman, N., Vesel, A., & Gunde, M. K. (2010). Colorimetric properties of reversible thermochromic printing inks. *Dyes and pigments*, *86*(3), 271-277.

2. Rauh, R. D. (1999). Electrochromic windows: an overview. *Electrochimica Acta*, *44*(18), 3165-3176.

3. Hwu, Y. R., Bai, C. C., Tao, L. C., Luo, D. G., & Hu, A. T. (1995). *U.S. Patent No. 5,422,181*. Washington, DC: U.S. Patent and Trademark Office.

4. Irie, M. (2006). *U.S. Patent No. 7,057,054*. Washington, DC: U.S. Patent and Trademark Office.

5. Nunes, D., Pimentel, A., Santos, L., Barquinha, P., Pereira, L., Fortunato, E., & Martins, R. (2018). Metal Oxide Nanostructures: Synthesis, Properties and Applications. Elsevier..

6. Dürr, H., & Bouas-Laurent, H. (Eds.). (2003). *Photochromism: molecules and systems*. Elsevier.

7. Santamouris, M. (2018). *Minimizing Energy Consumption, Energy Poverty and Global and Local Climate Change in the Built Environment: Innovating to Zero: Causalities and Impacts in a Zero Concept World*.

8. Garshasbi, S., & Santamouris, M. (2019). Using advanced thermochromic technologies in the built environment: Recent development and potential to decrease the energy consumption and fight urban overheating. *Solar Energy Materials and Solar Cells*, *191*, 21-32.

9. Santamouris, M. (2015). Regulating the damaged thermostat of the cities—Status, impacts, and mitigation challenges. *Energy and Buildings*, *91*, 43-56.

10. Santamouris, M. (2014). On the energy impact of urban heat island and global warming on buildings. *Energy and Buildings*, *82*, 100-113.

11. Santamouris, M. (2015). Analyzing the heat island magnitude and characteristics in one hundred Asian and Australian cities and regions. *Science of the Total Environment*, *512*, 582-598.

12. Akbari, H., Cartalis, C., Kolokotsa, D., Muscio, A., Pisello, A. L., Rossi, F., ... & Zinzi, M. (2016). Local climate change and urban heat island mitigation techniques–the state of the art. *Journal of Civil Engineering and Management*, *22*(1), 1-16.

13. Santamouris, M., Ding, L., Fiorito, F., Oldfield, P., Osmond, P., Paolini, R., & Synnefa, A. (2017). Passive and active cooling for the outdoor built environment–Analysis and assessment of the cooling potential of mitigation technologies using performance data from 220 large scale projects. *Solar Energy*, *154*, 14-33.

14. Akbari, H. (2003). Measured energy savings from the application of reflective roofs in two small non-residential buildings. Energy, 28(9), 953-967.

15. Saeli, M., Piccirillo, C., Parkin, I. P., Binions, R., & Ridley, I. (2010). Energy modelling studies of thermochromic glazing. Energy and Buildings, 42(10), 1666-1673.

16. Granqvist, C. G., Lansåker, P. C., Mlyuka, N. R., Niklasson, G. A., & Avendano, E. (2009). Progress in chromogenics: new results for electrochromic and thermochromic materials and devices. Solar Energy Materials and Solar Cells, 93(12), 2032-2039.

17. Raditoiu, A., Raditoiu, V., Nicolae, C. A., Raduly, M. F., Amariutei, V., & Wagner, L. E. (2016). Optical and structural dynamical behavior of Crystal Violet Lactone–Phenolphthalein binary thermochromic systems. Dyes and Pigments, 134, 69-76.

18. Tözüm, M. S., Aksoy, S. A., & Alkan, C. (2018). Microencapsulation of Three-Component Thermochromic System for Reversible Color Change and Thermal Energy Storage. Fibers and Polymers, 19(3), 660-669.

19. Malaiyandi, M. M., Sadar, H., Lee, P., & O'Grady, R. (1980). Removal of organics in water using hydrogen peroxide in presence of ultraviolet light. Water Research, 14(8), 1131-1135.

20. Zhang, W., Ji, X., Zeng, C., Chen, K., Yin, Y., & Wang, C. (2017). A new approach for the preparation of durable and reversible color changing polyester fabrics using thermochromic leuco dye-loaded silica nanocapsules. Journal of Materials Chemistry C, 5(32), 8169-8178.

21. Ye, X., Luo, Y., Gao, X., & Zhu, S. (2012). Design and evaluation of a thermochromic roof system for energy saving based on poly (N-isopropylacrylamide) aqueous solution. Energy and buildings, 48, 175-179.

22. Kuehni, Rolf G. Color: An Introduction to Practice and Principles. Hoboken, N.J., Wiley, 2012, pp. 4–5.

23. Perrier, A., Maurel, F., & Jacquemin, D. (2012). Single molecule multi photochromism with diarylethenes. *Accounts of chemical research*, *45*(8), 1173-1182.

24. Liu, M. N., Yan, X., You, M. H., Fu, J., Nie, G. D., Yu, M., ... & Long, Y. Z. (2018). Reversible photochromic nanofibrous membranes with excellent water/windproof and breathable performance. *Journal of Applied Polymer Science*, *135*(23), 46342.

25. Avella-Oliver, M., Morais, S., Puchades, R., & Maquieira, Á. (2016). Towards photochromic and thermochromic biosensing. *TrAC Trends in Analytical Chemistry*, *79*, 37-45.

26. Somani, P. R., & Radhakrishnan, S. (2003). Electrochromic materials and devices: present and future. *Materials chemistry and physics*, *77*(1), 117-133.

27. Avella-Oliver, M., Morais, S., Puchades, R., & Maquieira, Á. (2016). Towards photochromic and thermochromic biosensing. *TrAC Trends in Analytical Chemistry*, *79*, 37-45.

28. Xia, X. H., Tu, J. P., Zhang, J., Huang, X. H., Wang, X. L., Zhang, W. K., & Huang, H. (2009). Multicolor and fast electrochromism of nanoporous NiO/poly (3, 4-ethylenedioxythiophene) composite thin film. *Electrochemistry Communications*, *11*(3), 702-705.

29. Jittiarporn, P., Badilescu, S., Al Sawafta, M. N., Sikong, L., & Truong, V. V. (2017). Electrochromic properties of sol–Gel prepared hybrid transition metal oxides–A short review. *Journal of Science: Advanced Materials and Devices*, *2*(3), 286-300. Somani, P. R., & Radhakrishnan, S. (2003). Electrochromic materials and devices: present and future. *Materials chemistry and physics*, *77*(1), 117-133.

30. Somani, P. R., & Radhakrishnan, S. (2003). Electrochromic materials and devices: present and future. Materials chemistry and physics, 77(1), 117-133.

31. Fritsch, E., Massi, L., Rossman, G. R., Hainschwang, T., Jobic, S., & Dessapt, R. (2007). Thermochromic and photochromic behaviour of "chameleon" diamonds. Diamond and related materials, 16(2), 401-408.

32. Durasevic, V. (2016). Smart dyes for medical textiles. In Advances in Smart Medical Textiles (pp. 19-55). Woodhead Publishing.

33. Bourque, A. N., & White, M. A. (2014). Control of thermochromic behaviour in crystal violet lactone (CVL)/alkyl gallate/alcohol ternary mixtures. *Canadian Journal of Chemistry*, *93*(1), 22-31.

34. Bourque, A. N., & White, M. A. (2014). Control of thermochromic behaviour in crystal violet lactone (CVL)/alkyl gallate/alcohol ternary mixtures. *Canadian Journal of Chemistry*, *93*(1), 22-31.

35. Muthyala, R. A. M. A. I. A. H., & Lan, X. I. A. N. G. F. U. (1997). *The Chemistry of Leuco Triarylmethanes* (p. 125). Plenum Press: New York.

36. Zhang, P., Xiao, X., & Ma, Z. W. (2016). A review of the composite phase change materials: Fabrication, characterization, mathematical modeling and application to performance enhancement. *Applied Energy*, *165*, 472-510.

37. Akbari, H., Bretz, S., Kurn, D. M., & Hanford, J. (1997). Peak power and cooling energy savings of high-albedo roofs. *Energy and Buildings*, *25*(2), 117-126.

38. Nassau, K. (2001). The physics and chemistry of color: the fifteen causes of color. *The Physics and Chemistry of Color: The Fifteen Causes of Color, 2nd Edition, by Kurt Nassau, pp. 496. ISBN 0-471-39106-9. Wiley-VCH, July 2001*, 496.

39. *"Bubbles, Bubbles, Everywhere, But Not a Drop to Drink". The Lipid Chronicles. 11 November 2011. Archived from the original on 26 April 2012. Retrieved 1 August 2012.*

40. Stöber, W., Fink, A., & Bohn, E. (1968). Controlled growth of monodisperse silica spheres in the micron size range. *Journal of colloid and interface science*, *26*(1), 62-69.

41. Van Helden, A. K., Jansen, J. W., & Vrij, A. (1981). Preparation and characterization of spherical monodisperse silica dispersions in nonaqueous solvents. *Journal of Colloid and Interface Science*, *81*(2), 354-368.

42. Han, J., Yu, T., & Im, S. H. (2017). Synthesis of uniform silica particles with controlled size by organic amine base catalysts via one-step process. *Journal of industrial and engineering chemistry*, *52*, 376-381.

43. Panák, O., Držková, M., & Kaplanová, M. (2015). Insight into the evaluation of colour changes of leuco dye based thermochromic systems as a function of temperature. Dyes and Pigments, 120, 279-287.

44. Jay Bieber, SU70 SEM (2019). Retrieved from http://www.nrec.usf.edu/documents/tools/Hitachi%20SU70%20Scanning%20Electron%20Microscope.pdf

45. Geng, X., Li, W., Wang, Y., Lu, J., Wang, J., Wang, N., ... & Zhang, X. (2018). Reversible thermochromic microencapsulated phase change materials for thermal energy storage application in thermal protective clothing. *Applied energy*, *217*, 281-294.

46. Wang, S., Wang, X., Jia, B., & Jing, X. (2017). Fabrication and characterization of poly (bisphenol A borate) with high thermal stability. *Applied Surface Science*, *392*, 481-491.

47. Chen, M., Wu, L., Zhou, S., & You, B. (2006). A method for the fabrication of monodisperse hollow silica spheres. *Advanced materials*, *18*(6), 801-806.

Appendix A: Detail of EDS Mapping for BDTCM at SiO$_2$
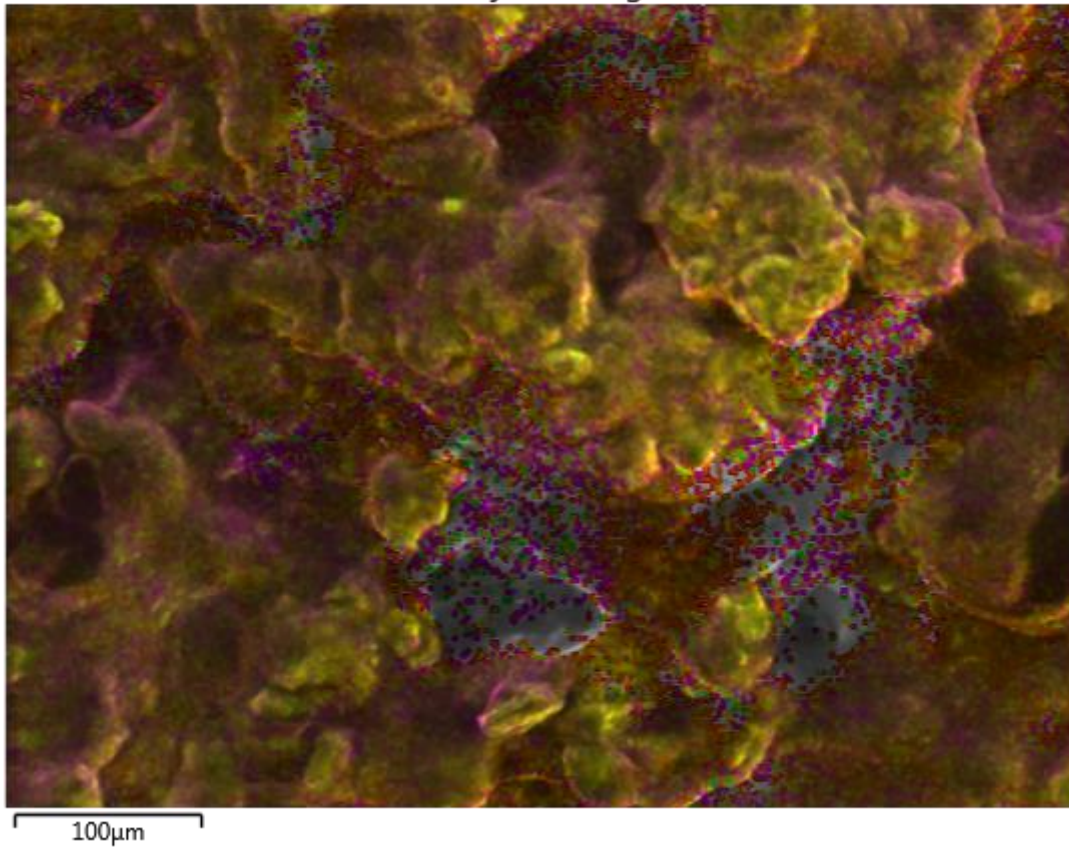
Figure A.1 EDS mapping of the BDTCM at SiO2 sample

C Kα1_2

Na Kα1_2

100μm

100μm

O Kα1

Si Kα1

100μm

100μm

P Kα1

S Kα1

100μm

100μm
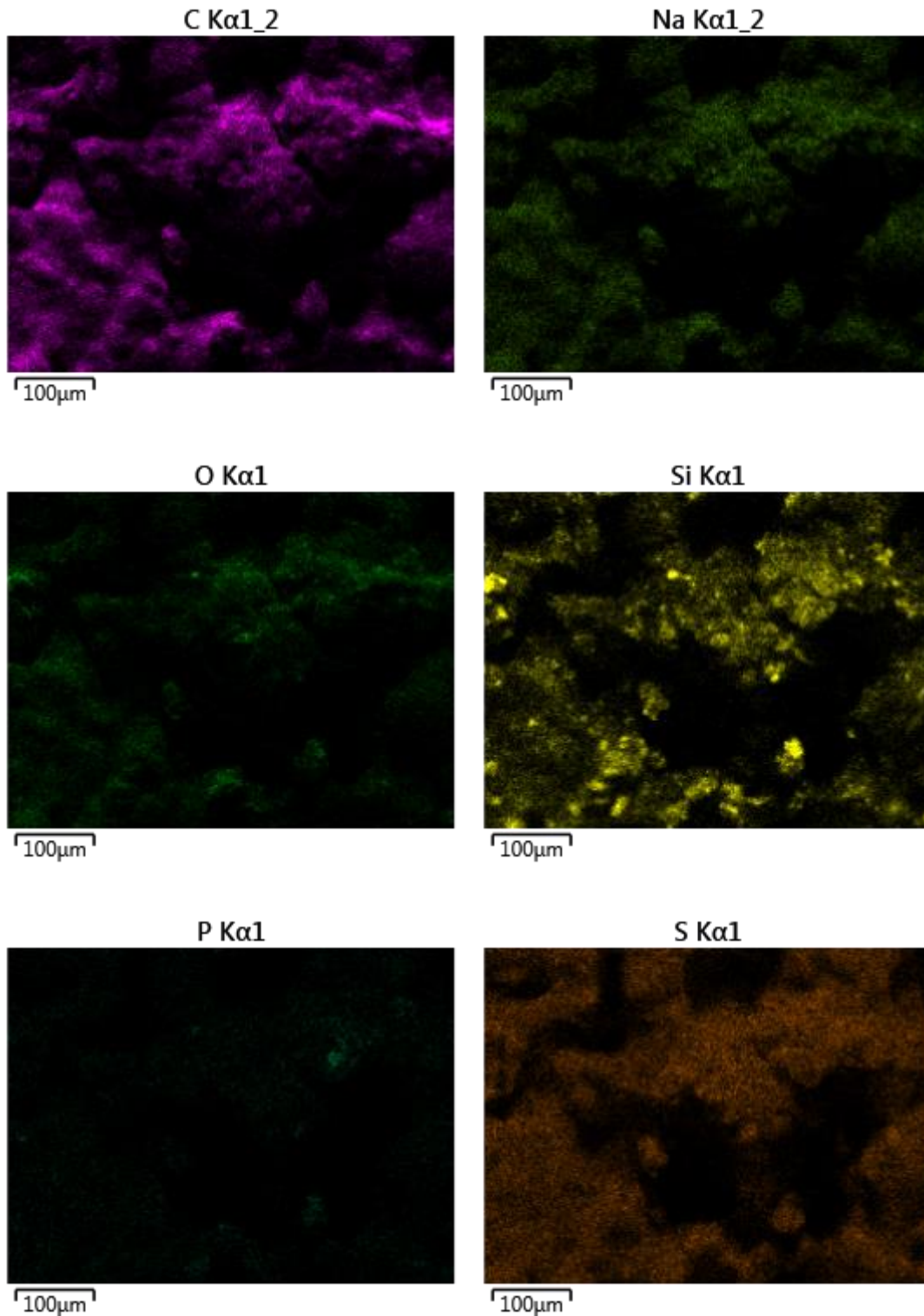
Figure A.2 EDS different elements mapping of the BDTCM at SiO2 sample

Appendix B: Detail of DLS Results

System

Temperature (°C):	20.0	Duration Used (s):	60
Count Rate (kcps):	370.7	Measurement Position (mm):	4.65
Cell Description:	Disposable sizing cuvette	Attenuator:	10

Results

			Size (d.nm):	% Intensity:	St Dev (d.n...
Z-Average (d.nm):	2186	Peak 1:	2287	98.7	1034
PdI:	0.257	Peak 2:	520.7	1.3	102.1
Intercept:	0.828	Peak 3:	0.000	0.0	0.000
Result quality :	Refer to quality report				
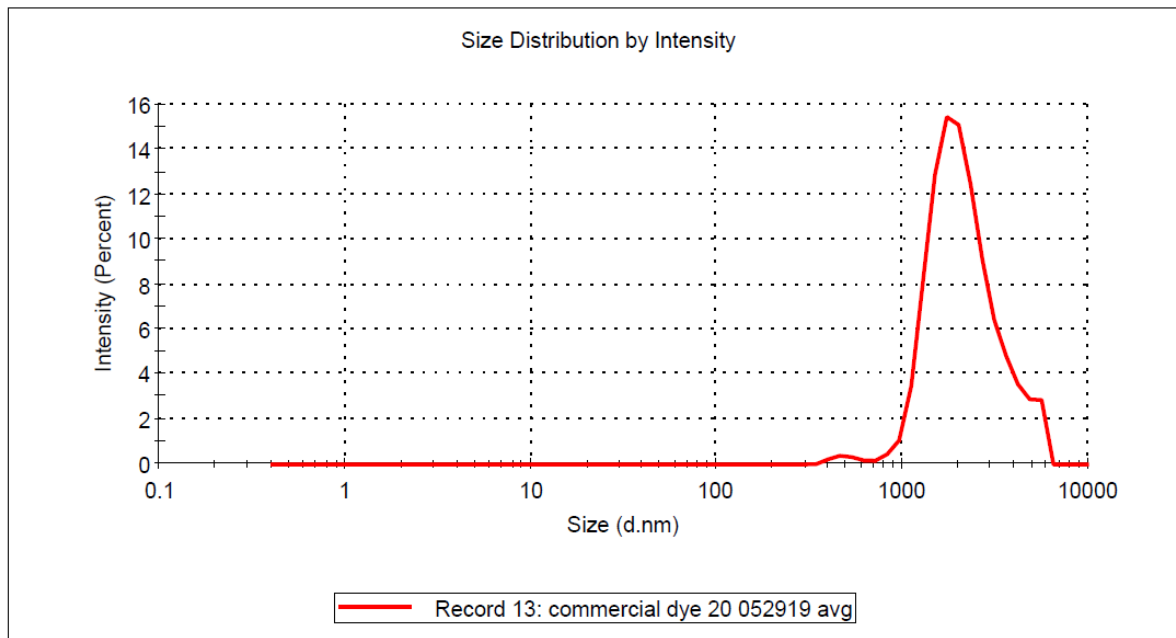
Figure B.1 Average particle size of commercial dye at 20 degrees C

52

Temperature (°C):	30.1	Duration Used (s):	60
Count Rate (kcps):	483.5	Measurement Position (mm):	4.65
Cell Description:	Disposable sizing cuvette	Attenuator:	10

Results

			Size (d.nm):	% Intensity:	St Dev (d.n...
Z-Average (d.nm):	2014	Peak 1:	1723	89.7	416.3
PdI:	0.249	Peak 2:	4544	10.3	870.6
Intercept:	0.847	Peak 3:	0.000	0.0	0.000
Result quality :	Refer to quality report				

Figure B.2 Average particle size of commercial dye at 30 degrees C

53

System

Temperature (°C):	40.0	Duration Used (s):	60
Count Rate (kcps):	271.1	Measurement Position (mm):	4.65
Cell Description:	Disposable sizing cuvette	Attenuator:	9

Results

			Size (d.nm):	% Intensity:	St Dev (d.n...
Z-Average (d.nm):	1896	Peak 1:	1864	100.0	360.0
Pdl:	0.099	Peak 2:	0.000	0.0	0.000
Intercept:	0.903	Peak 3:	0.000	0.0	0.000
Result quality :	Refer to quality report				

Figure B.3 Average particle size of commercial dye at 40 degrees C

System

Temperature (°C):	20.0	Duration Used (s):	70
Count Rate (kcps):	169.6	Measurement Position (mm):	4.65
Cell Description:	Disposable sizing cuvette	Attenuator:	9

Results

			Size (d.nm):	% Intensity:	St Dev (d.n...
Z-Average (d.nm):	2443	Peak 1:	1818	90.6	620.3
PdI:	0.310	Peak 2:	5100	9.4	537.3
Intercept:	0.876	Peak 3:	0.000	0.0	0.000
Result quality :	Refer to quality report				
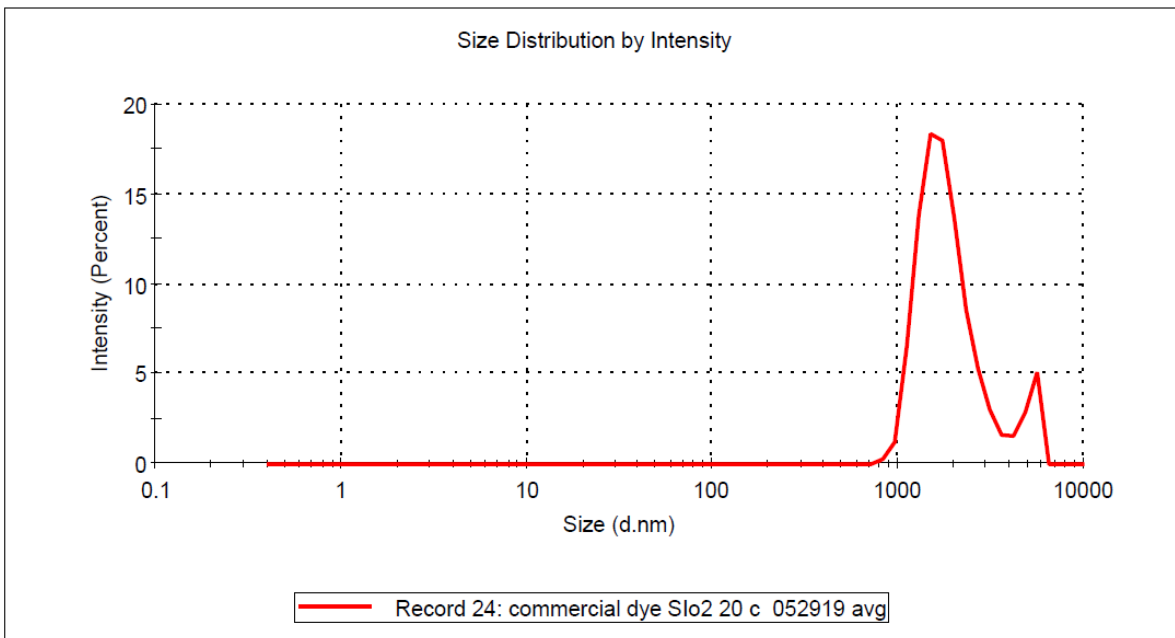
Figure B.4 Average particle size of commercial dye with SiO2 at 20 degrees C

System

Temperature (°C):	30.0	Duration Used (s):	70
Count Rate (kcps):	236.2	Measurement Position (mm):	4.65
Cell Description:	Disposable sizing cuvette	Attenuator:	9

Results

				Size (d.nm):	% Intensity:	St Dev (d.n...
Z-Average (d.nm):	2665	Peak 1:		2472	100.0	630.5
PdI:	0.242	Peak 2:		0.000	0.0	0.000
Intercept:	0.907	Peak 3:		0.000	0.0	0.000
Result quality :	Good					

Size Distribution by Intensity

Record 20: commercial dye SIo2 30 c 052919 avg

Figure B.5 Average particle size of commercial dye with SiO2 at 30 degrees C

System

Temperature (°C):	40.0	Duration Used (s):	60
Count Rate (kcps):	288.6	Measurement Position (mm):	4.65
Cell Description:	Disposable sizing cuvette	Attenuator:	9

Results

			Size (d.nm):	% Intensity:	St Dev (d.n...
Z-Average (d.nm):	2445	Peak 1:	1935	99.6	439.5
PdI:	0.328	Peak 2:	5560	0.4	6.104e-5
Intercept:	0.929	Peak 3:	0.000	0.0	0.000
Result quality :	Refer to quality report				

Figure B.6 Average particle size of commercial dye with SiO2 at 40 degrees C

57

www.manaraa.com

System

Temperature (°C):	20.0	Duration Used (s):	60
Count Rate (kcps):	377.5	Measurement Position (mm):	4.65
Cell Description:	Disposable sizing cuvette	Attenuator:	10

Results

			Size (d.nm):	% Intensity:	St Dev (d.n...
Z-Average (d.nm):	385.7	Peak 1:	559.5	98.9	405.4
Pdl:	0.445	Peak 2:	5055	1.1	578.9
Intercept:	0.911	Peak 3:	0.000	0.0	0.000
Result quality :	Good				

Figure B.7 Average particle size of blue dye with SiO2 at 20 degrees C

System

Temperature (°C):	30.0	Duration Used (s):	60
Count Rate (kcps):	357.9	Measurement Position (mm):	4.65
Cell Description:	Disposable sizing cuvette	Attenuator:	10

Results

			Size (d.nm):	% Intensity:	St Dev (d.n...
Z-Average (d.nm):	429.6	Peak 1:	521.4	86.9	225.1
PdI:	0.404	Peak 2:	127.2	11.9	33.23
Intercept:	0.921	Peak 3:	5037	1.2	589.6
Result quality :	Good				
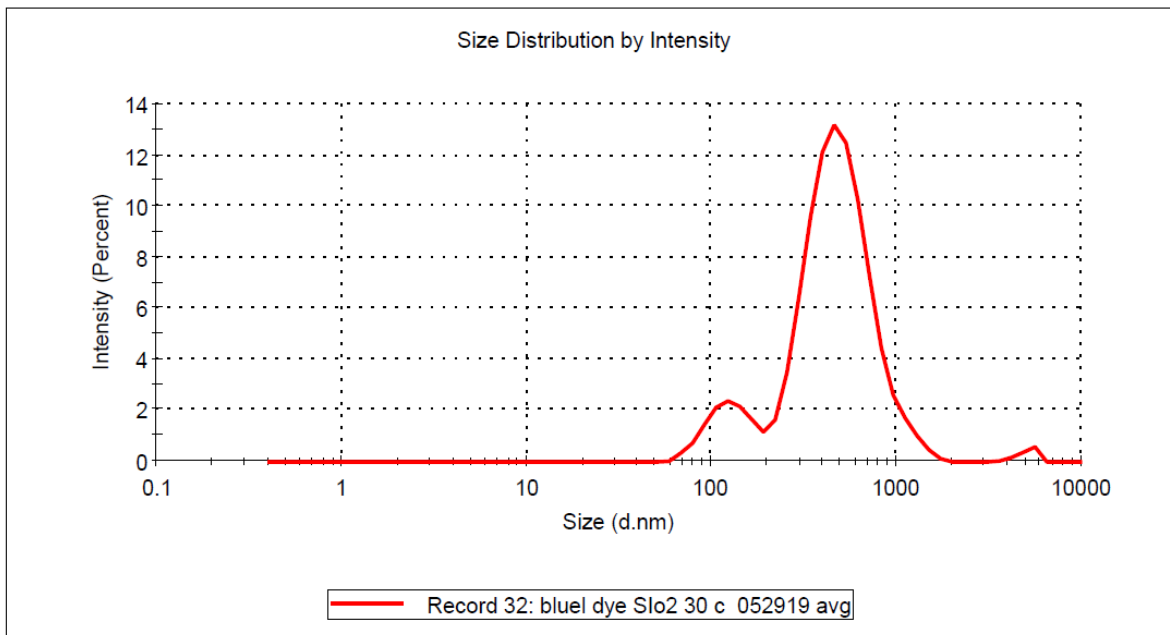
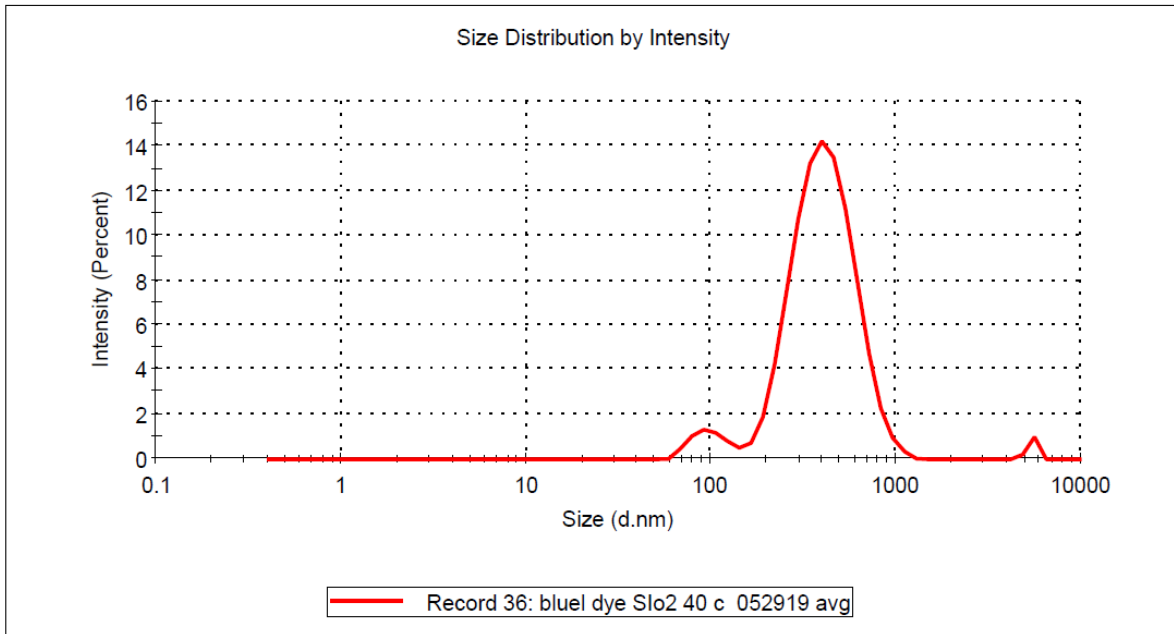Figure B.8 Average particle size of blue dye with SiO2 at 30 degrees C

Figure B.9 Average particle size of blue dye with SiO2 at 40 degrees C

60

Appendix C: Copyright Permissions

The permission below is for the use of material in Chapter 1.

This Agreement between Home -- Mingyang Huang ("You") and Elsevier ("Elsevier") consists of your license details and the terms and conditions provided by Elsevier and Copyright Clearance Center.

printable details

License Number	4642141437964
License date	Aug 04, 2019
Licensed Content Publisher	Elsevier
Licensed Content Publication	Elsevier Books
Licensed Content Title	Metal Oxide Nanostructures
Licensed Content Author	Daniela Nunes,Ana Pimentel,Lidia Santos,Pedro Barquinha,Luis Pereira,Elvira Fortunato,Rodrigo Martins
Licensed Content Date	Jan 1, 2019
Licensed Content Pages	45
Type of Use	reuse in a thesis/dissertation
Portion	figures/tables/illustrations
Number of figures/tables/illustrations	1
Format	electronic
Are you the author of this Elsevier chapter?	No
Will you be translating?	No
Original figure numbers	figure 1
Title of your thesis/dissertation	Encapsulation of Organic Thermochromic Materials with Silicon Dioxide
Expected completion date	Aug 2019
Estimated size (number of pages)	70
Publisher Tax ID	98-0397604

The permission below is for the use of material in Chapter 2.1.

This Agreement between Home -- Mingyang Huang ("You") and John Wiley and Sons ("John Wiley and Sons") consists of your license details and the terms and conditions provided by John Wiley and Sons and Copyright Clearance Center.

License Number	4612611224511
License date	Jun 19, 2019
Licensed Content Publisher	John Wiley and Sons
Licensed Content Publication	Wiley Books
Licensed Content Title	Sources of Color
Licensed Content Date	Oct 9, 2012
Licensed Content Pages	10
Type of use	Dissertation/Thesis
Requestor type	University/Academic
Format	Electronic
Portion	Figure/table
Number of figures/tables	1
Original Wiley figure/table number(s)	Figure 1.1
Will you be translating?	No
Title of your thesis / dissertation	Encapsulation of Organic Thermochromic Materials with Silicon Dioxide
Expected completion date	Aug 2019
Expected size (number of pages)	70
Publisher Tax ID	EU826007151

The permission below is for the use of material in Chapter 2.2.

This Agreement between Home -- Mingyang Huang ("You") and Elsevier ("Elsevier") consists of your license details and the terms and conditions provided by Elsevier and Copyright Clearance Center.

License Number	4642161430660
License date	Aug 04, 2019
Licensed Content Publisher	Elsevier
Licensed Content Publication	TrAC Trends in Analytical Chemistry
Licensed Content Title	Towards photochromic and thermochromic biosensing
Licensed Content Author	Miquel Avella-Oliver,Sergi Morais,Rosa Puchades,Ángel Maquieira
Licensed Content Date	May 1, 2016
Licensed Content Volume	79
Licensed Content Issue	n/a
Licensed Content Pages	9
Type of Use	reuse in a thesis/dissertation
Portion	figures/tables/illustrations
Number of figures/tables/illustrations	1
Format	electronic
Are you the author of this Elsevier article?	No
Will you be translating?	No
Title of your thesis/dissertation	Encapsulation of Organic Thermochromic Materials with Silicon Dioxide
Expected completion date	Aug 2019
Estimated size (number of pages)	70
Publisher Tax ID	98-0397604

The permission below is for the use of material in Chapter 2.3.

This Agreement between Home -- Mingyang Huang ("You") and Elsevier ("Elsevier") consists of
your license details and the terms and conditions provided by Elsevier and Copyright Clearance
Center.

License Number	4642170106196
License date	Aug 04, 2019
Licensed Content Publisher	Elsevier
Licensed Content Publication	Materials Chemistry and Physics
Licensed Content Title	Electrochromic materials and devices: present and future
Licensed Content Author	Prakash R. Somani,S. Radhakrishnan
Licensed Content Date	Jan 2, 2003
Licensed Content Volume	77
Licensed Content Issue	1
Licensed Content Pages	17
Type of Use	reuse in a thesis/dissertation
Portion	figures/tables/illustrations
Number of figures/tables/illustrations	1
Format	electronic
Are you the author of this Elsevier article?	No
Will you be translating?	No
Title of your thesis/dissertation	Encapsulation of Organic Thermochromic Materials with Silicon Dioxide
Expected completion date	Aug 2019
Estimated size (number of pages)	70
Publisher Tax ID	98-0397604

The permission below is for the use of material in Chapter 3.

This Agreement between Home -- Mingyang Huang ("You") and Elsevier ("Elsevier") consists of your license details and the terms and conditions provided by Elsevier and Copyright Clearance Center.

License Number	4642160777699
License date	Aug 04, 2019
Licensed Content Publisher	Elsevier
Licensed Content Publication	Journal of Industrial and Engineering Chemistry
Licensed Content Title	Synthesis of uniform silica particles with controlled size by organic amine base catalysts via one-step process
Licensed Content Author	Jin Han,Taekyung Yu,Sang Hyuk Im
Licensed Content Date	Aug 25, 2017
Licensed Content Volume	52
Licensed Content Issue	n/a
Licensed Content Pages	6
Type of Use	reuse in a thesis/dissertation
Portion	figures/tables/illustrations
Number of figures/tables/illustrations	1
Format	electronic
Are you the author of this Elsevier article?	No
Will you be translating?	No
Title of your thesis/dissertation	Encapsulation of Organic Thermochromic Materials with Silicon Dioxide
Expected completion date	Aug 2019
Estimated size (number of pages)	70
Publisher Tax ID	98-0397604

The permission below is for the use of material in Chapter 2.4